


Cite this: *RSC Adv.*, 2024, 14, 1304

Synthesis of triazole bridged *N*-glycosides of pyrazolo[1,5-*a*]pyrimidinones as anticancer agents and their *in silico* docking studies†

Ghanshyam Tiwari,^a Vinay Kumar Mishra,^a Priti Kumari,^a Ashish Khanna,^a Sunil Sharma^b and Ram Sagar ^{*ab}

In the pursuit of novel therapeutic agents, we present a comprehensive study on the design, synthesis, and evaluation of a diverse library of triazole bridged *N*-glycosides of pyrazolo[1,5-*a*]pyrimidinones, employing a microwave-assisted synthetic approach via 'click chemistry'. This methodology offers efficient and accelerated access to the glycohybrids, showcasing improved reaction conditions that yield high-quality products. In this research endeavor, we have successfully synthesized a series of twenty-seven triazole bridged *N*-glycosides of pyrazolo[1,5-*a*]pyrimidinones. Our investigation extends beyond synthetic endeavors to explore the potential therapeutic relevance of these compounds. We subjected them to rigorous *in vitro* screening against prominent breast cancer cell lines MCF-7, MDA-MB231, and MDA-MB453. Among the library of compounds synthesized, (2*S*,3*S*,4*R*,5*S*,6*S*)-2-(acetoxymethyl)-6-(4-((5-(4-methoxyphenyl)-7-oxopyrazolo[1,5-*a*]pyrimidin-1(7*H*)-yl)methyl)-1*H*-1,2,3-triazol-1-yl)tetrahydro-2*H*-pyran-3,4,5-triyl triacetate emerged as a potent compound, exhibiting remarkable anti-cancer activity with an IC₅₀ value of 27.66 μM against the MDA-MB231 cell line. Additionally, (2*S*,3*R*,4*R*,5*S*,6*S*)-2-(acetoxymethyl)-6-(4-((7-oxo-5-(4-(trifluoromethyl)phenyl)pyrazolo[1,5-*a*]pyrimidin-1(7*H*)-yl)methyl)-1*H*-1,2,3-triazol-1-yl)tetrahydro-2*H*-pyran-3,4,5-triyl triacetate displayed notable inhibitory potential against the MCF-7 cell line, with an IC₅₀ value of 4.93 μM. Furthermore, *in silico* docking analysis was performed to validate our experimental findings. These findings underscore the promise of our triazole bridged *N*-glycosides of pyrazolo[1,5-*a*]pyrimidinones as potential anti-cancer agents. This research not only enriches the field of glycohybrid synthesis but also contributes valuable insights into the development of novel anti-cancer therapeutics.

Received 14th October 2023
Accepted 18th December 2023

DOI: 10.1039/d3ra06993a

rsc.li/rsc-advances

1. Introduction

N-heterocycles occupy a pivotal position in the chemical reactions occurring within every living organism, serving as essential components for the construction of RNA and DNA.¹ Researchers have shown significant interest in *N*-heterocyclic organic compounds, particularly the pyrazolo[1,5-*a*]pyrimidinones nucleus, due to their potential applications in various fields, including medicine and materials science.^{2,3} This class of compounds consists of a pyrazole ring fused to a pyrimidine ring, with a ketone functional group of the pyrazolo[1,5-*a*]pyrimidine ring system.⁴ Studies have focused on the potential of pyrazolo[1,5-*a*]pyrimidinone derivatives as therapeutic agents, particularly as inhibitors of enzymes such as

cyclin-dependent kinases (CDKs)⁵ and phosphodiesterases (PDEs),⁶ which play a crucial role in various diseases such as cancer,⁷ asthma,⁷ chronic obstructive pulmonary disease (COPD), and erectile dysfunction.^{8–13} In addition to their potential as therapeutic agents, pyrazolo[1,5-*a*]pyrimidinones have also been explored for their use in organic electronics due to their electronic properties, which include their ability to act as electron transport materials and their potential for use in optoelectronic devices.^{14–17} Hence, the synthesis of small compounds possessing drug-like characteristics has held central importance for medicinal chemists. In this context, glycosylation can play a crucial role in the advancement of novel pharmaceuticals.

Glycosylation is a vital process involving the attachment of glycone molecules to bioactive aglycone molecules, resulting in the formation of novel glycosides.^{18–22} This technique finds widespread application in drug development, with the aim of improving the pharmacological properties and ADMET (Absorption, Distribution, Metabolism, Excretion, and Toxicity) parameters of drugs.²³ Notable instances of successful glycosylation in drug development include the glycosylated forms of paclitaxel^{24,25}

^aDepartment of Chemistry, Institute of Science, Banaras Hindu University, Varanasi, 221005, India. E-mail: ram.sagar@jnu.ac.in

^bGlycochemistry Laboratory, School of Physical Sciences, Jawaharlal Nehru University, New Delhi, 110067, India

† Electronic supplementary information (ESI) available. See DOI: <https://doi.org/10.1039/d3ra06993a>



and demethylepipodophyllotoxin,^{26,27} both of which exhibit increased water solubility and reduced toxicity. Additionally, glycosylated diphyllin²⁸ has demonstrated enhanced potency as a topoisomerase II inhibitor compared to its parent compound. Furthermore, the incorporation of acyl-protected sugar units into etopophos (tafluposide) has been shown to augment its biological activity when contrasted with etopophos in isolation.²⁹ Consequently, the amalgamation of the pharmacophoric moiety (N-heterocycles) with the glycone unit through glyco-conjugation has proven to be an effective approach for the treatment of rapidly proliferating cancer cells.^{30,31}

Triazole linked *N*-glycosides have also been extensively studied as potential drug candidates, with diverse pharmacological activities such as antifungal, antibacterial, antiviral, anticancer, and antitubercular agents.^{19,20,32–34} Triazole-based compounds have been used as pesticides,¹⁸ have unique properties such as mechanical strength,³⁵ electrical conductivity,³⁵ and bioremediation.^{36,37} These compounds show high affinity for metal ions and their ability to form stable coordination complexes with metals.^{31,38–40}

There are some bioactive scaffolds with various medicinal properties having the core moiety pyrazolopyrimidine and pyrazolo-pyrimidinone listed in Fig. 1. These scaffolds (A–F) show various biological potential and used as a treatment of various disorders in human such as, (A) formycin is used as antibacterial agent, (B) sildenafil is used as a treatment of erectile dysfunction, (C) oxoformycin act as antibacterial, (D) zaleplon is a hypnotic drug generally used as a treatment of the sleeping disorder (Insomnia) in human (E) Cox-2 inhibitor act as an anti-inflammatory agent which can be used as a treatment of arthritis (Fig. 1).^{41–43} Thus, the synthesis of small molecules with drug-like properties has been a focal point for medicinal chemists due to their significant role in the development of new drugs. So, inspired from these all we have designed triazole bridged *N*-glycosides of pyrazolo[1,5-*a*]pyrimidinones as glycohybrid (F).

In our previous study, we have discussed about the synthesis of a diverse library of *O*-propargylated pyrazolo[1,5-*a*]pyrimidines synthesized from diverse acetophenones as starting

material.⁴⁴ In the previous synthetic studies, *N*-propargylated pyrazolo[1,5-*a*]pyrimidinone was obtained as minor product. We have aimed to synthesize *N*-propargylated pyrazolo[1,5-*a*]pyrimidinone as a major product. Thus, here in this study, we have designed and efficiently synthesized a diverse library of *N*-propargylated pyrazolo[1,5-*a*]pyrimidinone as a major product by identifying better optimized reaction conditions and different synthetic protocol. Further, we have focused on the development of triazole bridged *N*-glycosides of pyrazolo[1,5-*a*]pyrimidinone compounds as glycohybrids and look for their anti-cancer activity against prominent breast cancer cell lines, MCF-7, MDA-MB231, and MDA-MB453. Furthermore, *in silico* docking studies were performed to validate our experimental findings. These detailed studies are reported in this paper.

2. Results and discussion

2.1. Synthesis

In our previous study, we synthesized a diverse library of triazole-linked glycohybrids of pyrazolo[1,5-*a*]pyrimidines obtained from *O*-propargylated pyrazolo[1,5-*a*]pyrimidines. While synthesizing *O*-propargylated pyrazolo[1,5-*a*]pyrimidines from various pyrazolopyrimidin-7-ols in DMF using K₂CO₃ and propargyl bromide, *N*-propargylated pyrazolo[1,5-*a*]pyrimidinones obtained as minor products. As, in several reports, it was found that triazole based *N*-glycosides exhibited diverse pharmacological properties and were extensively studied as potential drug candidates. Therefore, in interest to develop various triazole-linked *N*-glycosides, we designed and aimed to synthesize *N*-propargylated pyrazolo[1,5-*a*]pyrimidinones from propargylation of various pyrazolopyrimidin-7-ols under different reaction conditions. We devised a different synthetic route to obtain *N*-propargylated pyrazolo[1,5-*a*]pyrimidinones as a major product.

The present study on *N*-propargylation commenced with the treatment of pyrazolopyrimidin-7-ol **1** with propargyl bromide using K₂CO₃ as a base in DMF solvent at rt which afforded the products **10** and **10a** in 15% and 20% respectively (Table 1, entry 1). Further similar reaction was performed and heated at 60 °C, and it was observed that the *O*-propargylated product was major (75%) and the *N*-propargylated product was minor (20%) (Table 1, entry 2).

Aiming for improved results of *N*-propargylation, various solvents were screened such as DMF, THF, 1,4-dioxane, and acetone. Along with the solvents, various bases were also screened to improve the results and we discovered that 1,4-dioxane was the best solvent with K₂CO₃ base at 60 °C, afforded the 65% isolated yield of *N*-propargylated product **10** (Table 1, entry 7). The reaction optimization, and the results are summarized in Table 1.

Having the optimized conditions in our hands, we then focused our attention on the substrate scope. We utilized the diverse pyrazolopyrimidin-7-ol **1–9** as substrates, (synthesized by condensation of various β-keto esters and 3-amino pyrazole discussed in ESI†) to transform it into the diverse library of *N*-propargylated pyrazolo[1,5-*a*]pyrimidinones **10–18** using best optimized conditions treated with propargyl bromide, employing K₂CO₃ as a base in 1,4-dioxane (Scheme 1).

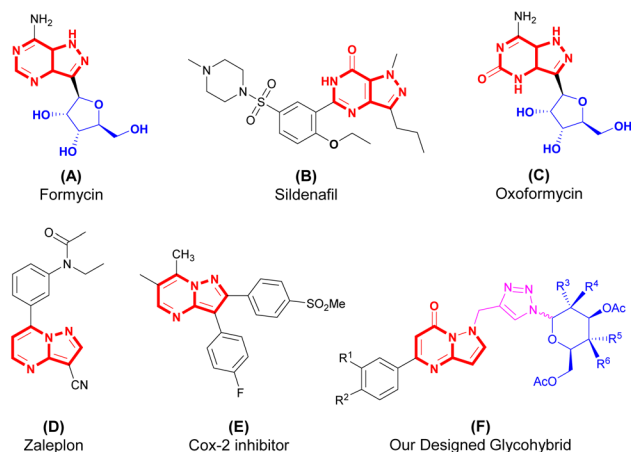
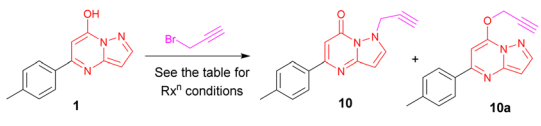


Fig. 1 Pyrazolo-pyrimidine based privileged scaffolds (A–F): (A) formycin, antibacterial, (B) Sildenafil, treatment of erectile dysfunction (C) oxoformycin, antibacterial drug (D) Zaleplon, anti-Insomnia drug, (E) Cox-2 inhibitor, anti-inflammatory agent, (F) our designed molecule.

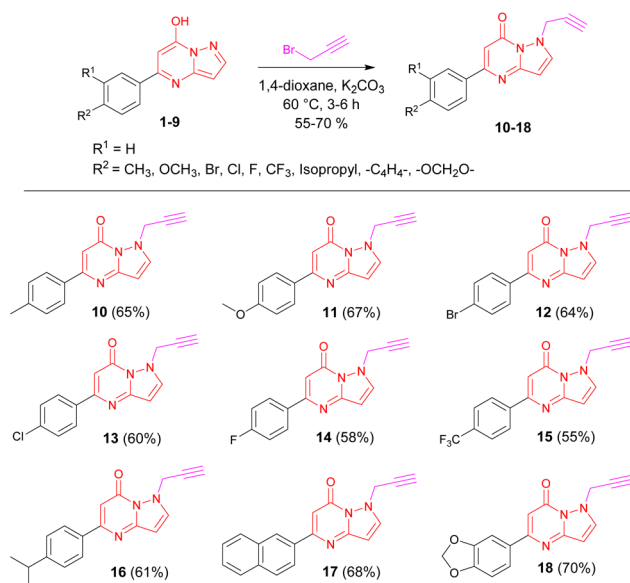
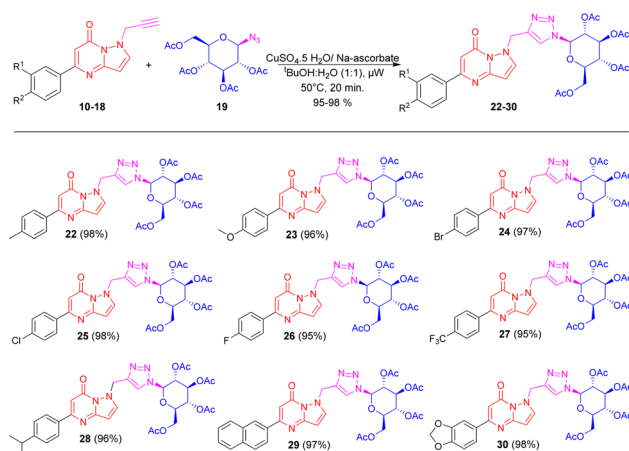
Table 1 Reaction optimization for synthesis of *N*-propargylated pyrazolo[1,5-*a*]pyrimidinone


Entry	Reaction conditions ^a	10 yield ^b (%)	10a yield ^b (%)
1	DMF, K ₂ CO ₃ , rt, 12 h	15	20
2	DMF, K ₂ CO ₃ , 60 °C, 3 h	20	75
3	DMF, NaH, 0 °C – rt, 3–6 h	30	40
4	THF, K ₂ CO ₃ , 60 °C, 3 h	NR	NR
5	THF, NaH, 0 °C, rt, 3 h	NR	NR
6	1,4-Dioxane, K ₂ CO ₃ , rt, 3 h	45	30
7	1,4-Dioxane, K₂CO₃, 60 °C, 3 h	65	30
8	1,4-Dioxane, Na ₂ CO ₃ , 60 °C, 3 h	55	45
9	1,4-Dioxane, Cs ₂ CO ₃ , 60 °C, 3 h	47	44
10	Acetone, K ₂ CO ₃ , 50 °C, 3 h	40	58
11	Acetone, Na ₂ CO ₃ , 50 °C, 3 h	35	60

^a NR – no reaction, Experimental Conditions: 5-(*p*-tolyl)pyrazolo[1,5-*a*]pyrimidin-7-ol (**1**) 0.5 g (2.22 mmol), K₂CO₃ 0.36 g (2.652 mmol), 15 ml, propargyl bromide 0.22 ml (2.65 mmol), 60 °C, 3 h. ^b Isolated yield.

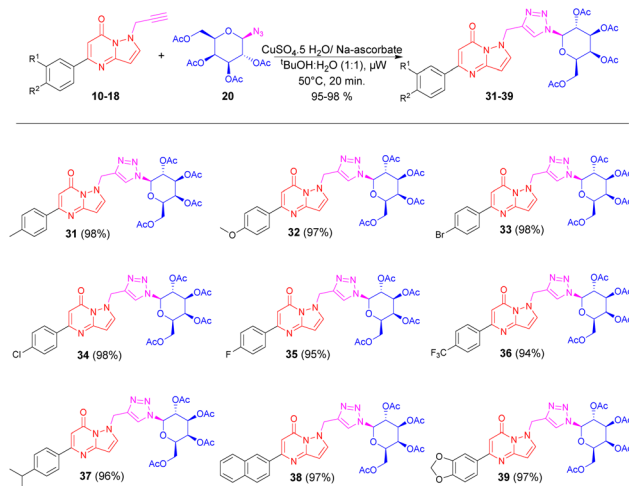
The azido-glycosides **19–21** were prepared by adopting similar reaction protocols as per reported methods (see the ESI† for synthetic method).¹⁸

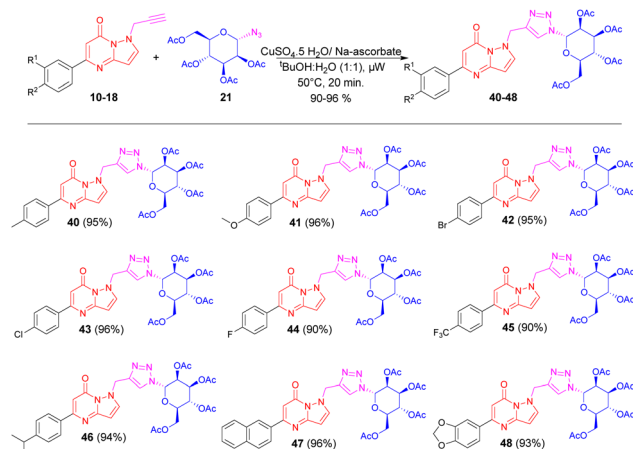
Having successful synthesis and complete characterization of both *N*-propargylated pyrazolo[1,5-*a*]pyrimidinones **10–18** and azido-glycosides **19–21**, it was focused to synthesize designed triazole bridged *N*-glycosides of pyrazolo[1,5-*a*]pyrimidinones.

**Scheme 1** Synthesis of *N*-propargylated pyrazolo[1,5-*a*]pyrimidinones **10–18**. In all cases, *O*-propargylated products were also formed as a minor product but the yields reported here are for *N*-propargylated products.**Scheme 2** Synthesis of triazole bridged *N*-glucosides **22–30**.

The initial click reaction between *N*-propargylated pyrazolo pyrimidinones **10** and azido-glucoside **19** took place under thermal conditions (50 °C) in *t*-BuOH-H₂O (1 : 1) for 6 hours, employing CuSO₄·5H₂O and sodium ascorbate which furnished the targeted product, triazole bridged *N*-glycoside pyrazolo[1,5-*a*]pyrimidinone, **22** with 80% isolated yield with some unreacted starting material. Subsequently, with the aim of expediting the reaction and enhancing product yields, the microwave irradiation technique was opted to obtain a good to excellent yield in a short reaction time. Thus, *N*-propargylated pyrazolo pyrimidinones **10** was reacted with 1-azido glucoside **19** in the presence of CuSO₄·5H₂O and sodium ascorbate in *t*-BuOH-H₂O (1 : 1, v/v) under microwave irradiation at 50 °C, which produces triazole bridged *N*-glucoside of pyrazolo[1,5-*a*]pyrimidinone **22** in excellent isolated yield (98%) (Scheme 2). Further, applying the above optimized reaction conditions under microwave irradiation, the triazole bridged *N*-glucosides of pyrazolo[1,5-*a*]pyrimidinone **22–30** were synthesized within a short period of time (20 min) in excellent yields (Scheme 2).

Applying a similar synthetic protocol using microwave irradiation conditions, we were also interested to synthesizing triazole

**Scheme 3** Synthesis of triazole bridged *N*-galactosides **31–39**.

Scheme 4 Synthesis of triazole bridged *N*-mannosides 40–48.

bridged *N*-galactosides *via* click reaction. Good to excellent isolated yields of triazole bridged *N*-galactosides of pyrazolo[1,5-*a*]pyrimidinones 31–39 were obtained, when *N*-propargylated pyrazolo[1,5-*a*]pyrimidinones 10–18 treated with 1-azido galactoside 20 in the presence of $\text{CuSO}_4 \cdot 5\text{H}_2\text{O}$ and sodium ascorbate in $t\text{BuOH-H}_2\text{O}$ (1:1, v/v) applying microwave irradiation under optimized reaction conditions (Scheme 3).

Further, we have extended our work to synthesize triazole bridged *N*-mannosides 40–48 *via* click chemistry approach. Herein we used a similar synthetic approach using microwave irradiation technique under optimized reaction conditions, where *N*-propargylated pyrazolo[1,5-*a*]pyrimidinones 10–18 were treated with 1-azido mannose 21 in the presence of $\text{CuSO}_4 \cdot 5\text{H}_2\text{O}$ and sodium ascorbate in $t\text{BuOH-H}_2\text{O}$ (1:1, v/v) using microwave irradiation under optimized reaction conditions, provides good to excellent isolated yield of triazole bridged *N*-mannosides 40–48 (Scheme 4).

2.2. Anticancer activity

After having synthesized the library of triazole-bridged *N*-glycosides of pyrazolo[1,5-*a*]pyrimidinones 22–48, they were

screened for their anticancer activity using different cell lines. The MTT assay was used to investigate the anticancer activity of twenty-seven synthesized compounds on the growth inhibition and decrement in cell viability of MDA-MB-231 (human breast cancer). Different concentrations were tested for a duration of 72 hours, and the results were compared to a control. Positive controls, namely YM155 and menadione, were also utilized, and the findings are presented in Fig. S2† and Table 2.

The results summarized in Table 2 showed moderate growth inhibition in all tested compounds with better activity with compounds 23, 26, 30, 33, 36 and 41 in MDA-MB231 breast cancer cells. These compounds show almost 50% inhibition at 25 μM concentration. These six compounds were further screened, and results were taken to find out IC_{50} values of these compounds (Fig. 2).

MDA-MB-231 represents a specific subtype, known as the triple negative breast cancer (TNBC). The investigation study was extended with active six hit compounds (23, 26, 30, 33, 36 and 41) in two other different cancer cell lines (MCF-7 and MDA-MB-453), each representing a separate class of breast cancers (MCF-7: hormone receptor/HR-positive; MDA-MB-453: human epidermal growth factor 2 receptor/HER2 positive). We also included normal mammary epithelial MCF-10A cells in our experiments to confirm if the growth-inhibitory activities of the selected compounds are truly cancer cell-specific. The activity data from MCF-7 & MDA-MB-453 cell lines (tested at 1, 10 and 25 μM) and activity data from MCF-10 A cell line (tested at 25, 50 and 100 μM) are summarized in Fig. S1† (ESI) and Table 3.

The results summarized in Table 3 showed better inhibition of cell viability was observed with compounds 23, 26, 30, 33, 36 and 41 at 25 μM in MCF-7 (hormone receptor/HR-positive breast cancer cells). These compounds show almost 50% inhibition at 25 μM concentration.

The IC_{50} values for the most active compounds 23, 26, 30, 33, 36 and 41 were calculated and presented in Fig. 3 against MDA-MB-231 breast cancer cell line was found 27.66, 54.85, 39.48, 45.98, 32.12 and 37.57 μM respectively.

Table 2 Anti-cancer activity results

Compounds	Cell viability (%) \pm SD			Compounds	Cell viability (%) \pm SD		
	50 μM	25 μM	10 μM		50 μM	25 μM	10 μM
22	85.37 \pm 4.16	87.49 \pm 6.74	92.40 \pm 5.38	36	41.20 \pm 1.26	46.10 \pm 3.32	70.37 \pm 5.36
23	34.32 \pm 5.29	49.03 \pm 9.19	65.14 \pm 8.53	37	78.74 \pm 2.56	80.51 \pm 8.96	85.23 \pm 3.50
24	98.54 \pm 2.89	100.13 \pm 8.93	100.25 \pm 8.01	38	67.70 \pm 10.82	89.59 \pm 9.91	92.04 \pm 8.31
25	86.22 \pm 9.22	93.24 \pm 1.96	98.58 \pm 2.25	39	97.50 \pm 1.88	98.25 \pm 0.34	101.28 \pm 9.67
26	54.56 \pm 5.61	59.98 \pm 8.47	76.61 \pm 9.76	40	91.74 \pm 9.12	92.81 \pm 7.09	99.05 \pm 7.70
27	74.75 \pm 7.02	89.80 \pm 8.75	93.24 \pm 8.51	41	44.18 \pm 4.11	54.28 \pm 6.12	66.70 \pm 8.21
28	69.46 \pm 17.69	99.07 \pm 3.51	102.13 \pm 8.51	42	75.55 \pm 8.45	78.52 \pm 6.58	81.32 \pm 7.65
29	88.43 \pm 7.36	81.48 \pm 2.58	89.10 \pm 4.09	43	71.36 \pm 10.49	95.16 \pm 10.62	99.50 \pm 10.20
30	42.82 \pm 5.04	55.17 \pm 7.06	86.58 \pm 3.36	44	89.57 \pm 6.27	90.13 \pm 6.77	98.41 \pm 3.62
31	78.81 \pm 10.40	88.47 \pm 6.73	81.68 \pm 8.36	45	86.98 \pm 1.10	91.06 \pm 6.00	96.84 \pm 5.85
32	72.48 \pm 6.24	86.20 \pm 8.63	92.51 \pm 9.39	46	83.54 \pm 7.27	75.49 \pm 4.44	80.63 \pm 4.70
33	46.98 \pm 4.91	63.28 \pm 6.32	66.70 \pm 8.23	47	81.53 \pm 5.45	89.82 \pm 2.22	101.77 \pm 9.28
34	73.04 \pm 2.62	76.76 \pm 2.43	78.46 \pm 2.43	48	92.89 \pm 9.08	93.31 \pm 3.60	96.45 \pm 4.91
35	75.33 \pm 6.17	78.62 \pm 10.05	82.40 \pm 9.97	YM155 (20 nM)	23.39 \pm 3.13		
Menadione (20 μM)	23.76 \pm 5.70						



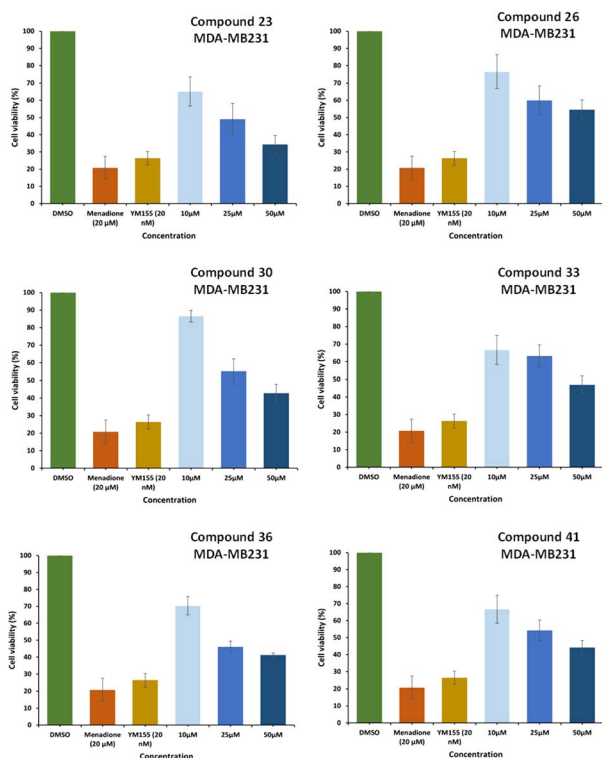


Fig. 2 Anti-cancer activity at different dilutions for active compounds were found at 10 μM , 25 μM , and 50 μM for compound 23, 26, 30, 33, 36 and 41 respectively compared to DMSO (control).

The IC_{50} values depicted in Fig. 4 for compound 23, 26, 30, 33, 36 and 41 against MCF-7 breast cancer cells line were found 9.24, 26.64, 18.49, 7.32, 4.93, 21.76 μM , respectively. While these compounds did not reach up to IC_{50} value against MDA-MB-453 cells. Furthermore, none of these compounds did have any growth inhibitory activity against normal breast epithelial cell (MCF-10A).

Thus, through screening against various cell lines such as MDA-MB231, MCF-7, MDA-MB453 and MCF-10A, it has been found that among the derived library of compounds, most of the compounds shows moderate to good anti-cancer activity. While compound 23 shows best inhibitory activity against MDA-

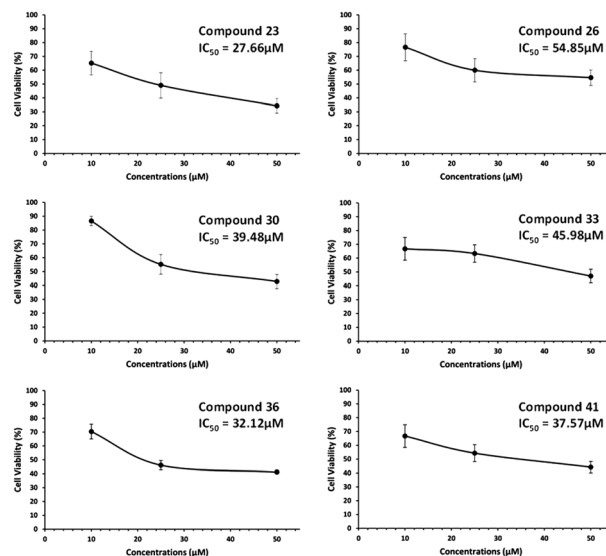


Fig. 3 IC_{50} of the most active compounds. To calculate half maximal inhibitory concentration (IC_{50}) of compounds 23, 26, 30, 33, 36 and 41 MDA-MB-231 cells were treated for 72 h with different concentrations (10, 25 and 50 μM) of the respective drugs and tested for cell viability by the MTT assay. IC_{50} values were determined by plotting values of percent cell viability against concentration of each of these compounds. IC_{50} values for compounds 23, 26, 30, 33, 36 and 41 against MDA-MB-231 breast cancer cell line were found 27.66, 54.85, 39.48, 45.98, 32.12, and 37.57 μM , respectively. The experiments were performed in triplicates, $n = 3$ and \pm SD value was calculated for each data point.

MB231 cell line with IC_{50} value at 27.66 μM and compound 36 shows best inhibitory activity against MCF-7 cell line with IC_{50} value of 4.93 μM .

2.3. Molecular docking studies

Various signaling pathways, nuclear hormone receptors such as estrogen receptors (ER), play a crucial role in leading normal breast development and mammary stem cells through regulating processes such as cell proliferation, cell death, differentiation, etc. These receptors are classified into two types, estrogen receptors alpha ($\text{ER-}\alpha$) and beta ($\text{ER-}\beta$), where $\text{ER-}\alpha$ serves as a key driver in oncogenic proliferation and

Table 3 Anti-cancer activity screening results

Compounds	Cell viability (%) \pm SD								
	MCF-7			MDA-MB-453			MCF-10A		
	25 μM	10 μM	1 μM	25 μM	10 μM	1 μM	25 μM	50 μM	100 μM
23	31.7 \pm 4.0	40.3 \pm 3.6	66.7 \pm 1.18	77.1 \pm 5.7	88.4 \pm 5.4	80.6 \pm 8.0	88.6 \pm 1.5	86.3 \pm 2.9	84.2 \pm 3.0
26	52.8 \pm 3.0	65.8 \pm 1.8	80.0 \pm 4.5	66.3 \pm 5.8	84.2 \pm 11.5	87.8 \pm 3.2	87.8 \pm 2.8	85.6 \pm 0.7	82.0 \pm 1.5
30	42.3 \pm 7.6	57.7 \pm 2.4	78.2 \pm 2.6	61.4 \pm 3.2	74.8 \pm 1.5	99.2 \pm 8.1	86.8 \pm 5.3	84.8 \pm 3.0	78.5 \pm 3.4
33	25.0 \pm 2.9	35.0 \pm 2.5	67.0 \pm 4.7	67.6 \pm 5.3	78.3 \pm 4.7	88.8 \pm 5.2	99.6 \pm 2.2	87.6 \pm 1.7	81.4 \pm 2.6
36	28.1 \pm 4.4	32.4 \pm 0.9	52.3 \pm 3.1	63.8 \pm 1.7	82.9 \pm 1.2	91.5 \pm 4.6	88.6 \pm 1.5	86.1 \pm 2.8	84.2 \pm 3.0
41	48.1 \pm 3.5	58.2 \pm 3.8	72.8 \pm 4.2	95.1 \pm 35.7	77.4 \pm 5.4	96.4 \pm 4.8	89.8 \pm 2.8	84.2 \pm 5.8	83.0 \pm 1.5
YM155 (20 nM)	31.2 \pm 1.7	31.2 \pm 1.7	31.2 \pm 1.7	36.2 \pm 1.5	36.2 \pm 1.5	36.2 \pm 1.5	39.2 \pm 1.6	39.2 \pm 1.6	39.2 \pm 1.6



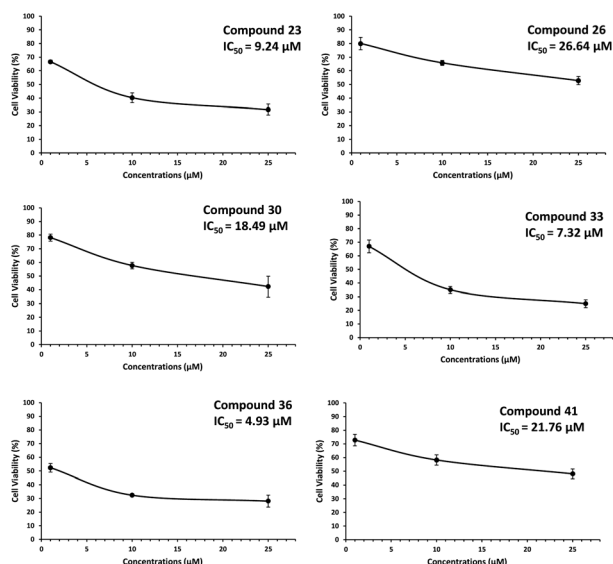


Fig. 4 IC_{50} of the most active compounds. To calculate half maximal inhibitory concentration (IC_{50}) of compounds 23, 26, 30, 33, 36 and 41 MCF-7 cells were treated for 72 h with different concentrations (10, 25 and 50 μ M) of the respective drugs and tested for cell viability by the MTT assay. IC_{50} values were determined by plotting values of percent cell viability against concentration of each of these compounds. The IC_{50} values for compound 23, 26, 30, 33, 36 and 41 against MCF-7 breast cancer cells line were found 9.24, 26.64, 18.49, 7.32, 4.93, 21.76 μ M, respectively. The experiments were performed in triplicates, $n = 3$ and \pm SD value was calculated for each data point.

metastasis. These protein receptors regulate the gene transcription within the cell nucleus by binding to related DNA regulatory regions and get overexpressed in case of breast cancer. Thus, ER- α , specifically, is gaining attention as a desirable target site for researchers to evaluate the potency of most anti-cancer and anti-proliferative drugs. The ER protein (PDB ID: 1A52) with ER- α (nuclear transcriptional factor) was selected and serves as the potential molecular target for the designed compounds in our investigation.

In several previous reports, it has been reported that heterocycle containing pyrazolo[1,5-*a*]pyrimidinone nucleus displays crucial drug like properties such as anticancer, anti-neoplastic, antiproliferative and many more. Thus, to identify the anticancer properties of pyrazolo[1,5-*a*]pyrimidinone nucleus, we performed molecular docking between the designed compounds with estrogen receptors (ER- α) protein (Protein Data Bank ID: 1A52).

Active site residues of the protein receptors have been identified as GLU353, ALA350, ASP351, TRP383, LEU387, LEU391, PHE404, HIS524, LEU525, LYS529, and TYR526. The parameters of the molecule in the active region were determined with the following values: grid box sizes of 30, 30, and 34 \AA^3 , and x , y , z centers of 97.977, 16.634, and 84.654 respectively. The docking study reveals that the interaction between synthesized triazole-bridged *N*-glycosides of pyrazolo[1,5-*a*]pyrimidinones and catalytic site ER- α protein occurs primarily through hydrogen bonds, hydrophobic bonds and π -stacking (as shown in Fig. 5).

Based on the docking results, the best docking poses, docking score with high binding affinity/energies and a number of favorable interactions suggest that most of the designed triazole-bridged *N*-glycosides of pyrazolo[1,5-*a*]pyrimidinones may serve as effective anti-cancer candidates. Among the derived library of compounds, compound 36 displays the best docking pose with binding energy $-43.51 \text{ kcal mol}^{-1}$ and glide score (-13.55) in mode 1 with minimum root mean square deviation value and perfectly fits into the active binding pocket of protein. In Fig. 6 four conventional hydrogen bonds were found between sugar moiety and TRP383, TYR526 active residues, respectively, and two conventional hydrogen bonds were found between triazole ring and oxygen atom of pyrimidinone ring with LYS529 active residue. Along with this π -anion interaction have been found between ASP351 active residue and pyrimidinone ring. Also, other interactions, such as alkyl and C-H interactions have also been found. These hydrophobic and hydrophilic interactions displayed the binding versatility of the designed molecules and the results obtained from *in silico* docking suggest that most of the molecules perfectly fit into the binding pocket of the docked protein and may possess anti-cancer activity.

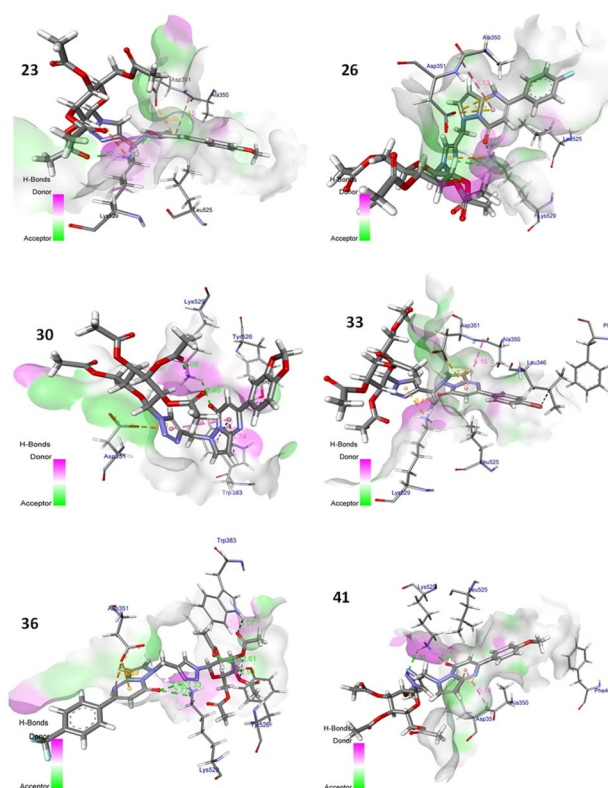


Fig. 5 Docking analysis of triazole-bridged *N*-glycosides of pyrazolo[1,5-*a*]pyrimidinones (compounds 23, 26, 30, 33, 36 and 41) and catalytic site of ER- α protein with 3D representation of hydrogen bond donor/acceptor surface (shown in pink and green colour) and hydrogen bond (green color). The docking analysis was conducted using the collected set of compounds (gray) into the proposed binding pocket of the X-ray crystallographic structure of ER- α protein (Protein Data Bank ID: 1A52, resolution: 2.6 \AA).



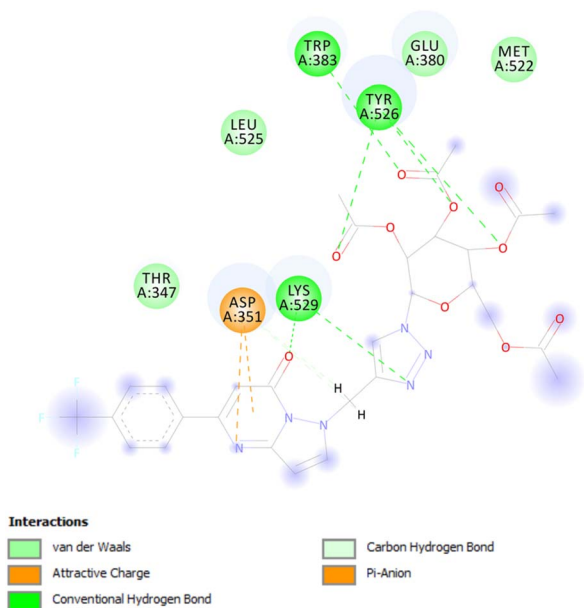


Fig. 6 2D representation of docked results of compound 36.

These results obtained from *in silico* studies further validate the biological potential of our designed molecules as an effective anti-cancer agent and support the results obtained from *in vitro* studies.

3. Conclusions

We have developed a series of triazole bridged *N*-glycosides of pyrazolo[1,5-*a*]pyrimidinones employed using microwave-assisted synthesis *via* 'click chemistry'. We have also optimized the reaction conditions for the synthesis of *N*-propargylated pyrazolo[1,5-*a*]pyrimidinone in good yields. Herein we have synthesized a series of twenty-seven diverse substituted triazole bridged *N*-glycosides of pyrazolo[1,5-*a*]pyrimidinones as glycohybrids, containing electron donating and electron withdrawing groups in a shorter reaction time. In this paper, we have also discussed about the anti-cancer property of synthesized triazole bridged *N*-glycosides of pyrazolo[1,5-*a*]pyrimidinones, through *in vitro* screening against MCF-7, MDA-MB231, and MDA-MB453 cell line culture. The *in silico* docking analysis was also been performed in support of the outcomes obtained from *in vitro* activity. We found that among the derived library of compounds, compound 23 shows the most potent anti-cancer activity with an IC_{50} value of 27.66 μ M against MDA-MB231 cell line and compound 36 shows the best inhibitory activity against MCF-7 cell line with IC_{50} value of 4.93 μ M.

4. Experimental section

4.1. General experimental methods

Anhydrous solvents and oven-dried glasswares were used to perform each experiment. CEM microwave synthesizer was used to carry out all the experiments. High resolution mass spectra

were recorded using an ESI source and a quadrupole/TOF mass spectrometer. Standard distillation methods were used to distill the solvents, which were then stored in 4 Å and 3 Å molecular sieves. ^1H (500 MHz), and ^{13}C (125 MHz) spectra were recorded with JEOL JNM-ECZ500R/S1 instrument. ^1H and ^{13}C chemical shifts are referenced to the solvents residual signals CDCl_3 ^1H NMR δ 7.26 and δ 77.16 for ^{13}C NMR, $\text{DMSO}-d_6$ ^1H NMR δ 2.5, and δ 39.52 for ^{13}C NMR reported in parts per million (ppm) at 25 °C. Coupling constants are expressed in hertz (Hz). Reactions were monitored by thin-layer chromatography carried out on 0.25 mm E. Merck silica gel plates (60F-254), spots were visualized by phosphomolybdic acid and 10% H_2SO_4 in ethanol. All reagents purchased from TCI, Merck and Sigma Aldrich *etc.*

4.2. Synthesis of triazole bridged *N*-glycosides of pyrazolo[1,5-*a*]pyrimidinones 22–48

The mixture of 300 mg (1.139 mmol) of 1-(prop-2-yn-1-yl)-5-(*p*-tolyl)pyrazolo[1,5-*a*]pyrimidin-7(1*H*)-one **10** and 425.34 mg (1.139 mmol) of azido glycoside of glucose **19** in 3 ml (1 : 1, v/v of H_2O - t -BuOH) of solvent, $\text{CuSO}_4 \cdot 5\text{H}_2\text{O}$ (1.42 mg, 0.0056 mmol) and sodium ascorbate (2.238 mg, 0.011 mmol) were added to it a microwave vial. The reaction mixture was subsequently microwave-heated for 20 minutes at 50 °C (100 W). TLC was used to verify that the reaction had finished. Water and ethyl acetate were used for extraction when the reaction was finished. To get the crude residue, the organic layer was dried over Na_2SO_4 and evaporated *via* a rotary evaporator. By using flash column chromatography to clean up the raw residue, pure compound **22** was obtained with a 98% isolated yield. Using similar methods, with 50 mg of propargylated reactants, the rest of the compounds **23–48** were synthesized in good to excellent yields, utilizing the azido glycosides of glucose, galactose, and mannose tetraacetate, respectively.

4.2.1 (2*S*,3*S*,4*R*,5*S*,6*S*)-2-(Acetoxymethyl)-6-(4-((5-oxo-5-(*p*-tolyl)pyrazolo[1,5-*a*]pyrimidin-1(7*H*)-yl)methyl)-1*H*-1,2,3-triazol-1-yl)tetrahydro-2*H*-pyran-3,4,5-triyl triacetate (22). Light yellow colored sticky solid; yield: 710.39 mg (98%), R_f = 0.21 (ethyl acetate); ^1H NMR (500 MHz, CDCl_3) δ 7.83 (s, 1H), 7.64 (s, 1H), 7.37 (d, J = 7.8 Hz, 2H), 7.30 (d, J = 7.6 Hz, 2H), 6.10 (s, 1H), 5.84 (s, 1H), 5.83 (d, J = 6.7 Hz, 1H), 5.39 (t, J = 9.5 Hz, 1H), 5.33 (t, J = 9.5 Hz, 1H), 5.20 (t, J = 10.0 Hz, 1H), 5.16–5.06 (m, 2H), 4.28 (dd, J = 12.7, 6.0 Hz, 1H), 4.12 (dd, J = 13.3 Hz, 2.5 Hz, 1H), 4.01–3.98 (m, 1H), 2.42 (s, 3H), 2.04 (s, 6H), 2.00 (s, 3H), 1.78 (s, 3H). ^{13}C NMR (125 MHz, CDCl_3) δ 170.4, 169.8, 169.4, 168.9, 156.2, 153.7, 143.5, 143.3, 142.6, 141.0, 129.9, 129.6, 128.6, 120.9, 100.1, 90.9, 85.9, 75.4, 72.4, 70.4, 67.8, 61.5, 45.7, 21.5, 20.7, 20.5, 20.5, 20.1. HRMS (ESI-TOF), m/z calcd. $\text{C}_{30}\text{H}_{33}\text{N}_6\text{O}_{10}$ [$M + \text{H}$] $^+$ 637.2253; found: 637.2573.

4.2.2 (2*S*,3*S*,4*R*,5*S*,6*S*)-2-(Acetoxymethyl)-6-(4-((5-(4-methoxyphenyl)-7-oxopyrazolo[1,5-*a*]pyrimidin-1(7*H*)-yl)methyl)-1*H*-1,2,3-triazol-1-yl)tetrahydro-2*H*-pyran-3,4,5-triyl triacetate (23). Light yellow colored powder; yield: 112.16 mg (96%), R_f = 0.22 (ethyl acetate); ^1H NMR (500 MHz, CDCl_3) δ 7.83 (s, 1H), 7.66 (s, 1H), 7.42 (d, J = 8.0 Hz, 2H), 7.00 (d, J = 9.3 Hz, 2H), 6.08 (s, 1H), 5.84 (d, J = 9.5 Hz, 1H), 5.83 (s, 1H), 5.39 (t, J = 8.5 Hz, 1H), 5.34 (t, J = 9.5 Hz, 1H), 5.20 (t, J = 10.0



Hz, 1H), 5.16–5.07 (m, 2H), 4.28 (dd, $J = 12.7, 5.0$ Hz, 1H), 4.13 (dd, $J = 12.0$ Hz, 2.5 Hz, 1H), 4.01–3.98 (m, 1H), 3.86 (s, 3H), 2.04 (s, 6H), 2.00 (s, 3H), 1.78 (s, 3H). ^{13}C NMR (125 MHz, CDCl_3) δ 170.5, 169.8, 169.4, 168.9, 161.4, 156.2, 153.5, 143.5, 143.3, 142.7, 130.3, 124.6, 120.9, 114.6, 100.2, 90.9, 85.9, 75.4, 72.4, 70.4, 67.7, 61.5, 55.5, 45.7, 20.7, 20.5, 20.5, 20.1. HRMS (ESI-TOF), m/z calcd. $\text{C}_{30}\text{H}_{33}\text{N}_6\text{O}_{11}$ $[\text{M} + \text{H}]^+$ 653.2202; found: 653.2532.

4.2.3 (2S,3S,4R,5S,6S)-2-(Acetoxymethyl)-6-(4-((5-(4-bromophenyl)-7-oxopyrazolo[1,5-*a*]pyrimidin-1(7*H*)-yl)methyl)-1*H*-1,2,3-triazol-1-yl)tetrahydro-2*H*-pyran-3,4,5-triyl triacetate (24). Brown colored sticky solid; yield: 100.60 mg (97%), $R_f = 0.23$ (ethyl acetate); ^1H NMR (500 MHz, CDCl_3) δ 7.83 (s, 1H), 7.72 (s, 1H), 7.64 (d, $J = 8.4$ Hz, 2H), 7.41 (d, $J = 8.8$ Hz, 2H), 6.09 (s, 1H), 5.84 (d, $J = 9.5$ Hz, 1H), 5.83 (s, 1H), 5.40 (t, $J = 9.0$ Hz, 1H), 5.33 (t, $J = 9.5$ Hz, 1H), 5.20 (t, $J = 9.5$ Hz, 1H), 5.10–5.03 (m, 2H), 4.28 (dd, $J = 12.7, 5.5$ Hz, 1H), 4.13 (dd, $J = 13.0$ Hz, 2.5 Hz, 1H), 4.02–3.98 (m, 1H), 2.04 (s, 6H), 2.01 (s, 3H), 1.79 (s, 3H). ^{13}C NMR (125 MHz, CDCl_3) δ 170.5, 169.8, 169.4, 169.0, 155.9, 152.4, 143.6, 143.2, 142.2, 132.5, 131.3, 130.4, 125.4, 121.0, 100.3, 91.0, 86.0, 75.4, 72.3, 70.5, 67.8, 61.5, 45.8, 20.8, 20.6, 20.5, 20.2. HRMS (ESI-TOF), m/z calcd. $\text{C}_{29}\text{H}_{30}\text{BrN}_6\text{O}_{10}$ $[\text{M} + \text{H}]^+$ 701.1201; found: 701.1566.

4.2.4 (2S,3S,4R,5S,6S)-2-(Acetoxymethyl)-6-(4-((5-(4-chlorophenyl)-7-oxopyrazolo[1,5-*a*]pyrimidin-1(7*H*)-yl)methyl)-1*H*-1,2,3-triazol-1-yl)tetrahydro-2*H*-pyran-3,4,5-triyl triacetate (25). Gray colored sticky solid; yield: 117.61 mg (98%), $R_f = 0.23$ (ethyl acetate); ^1H NMR (500 MHz, CDCl_3) δ 7.82 (s, 1H), 7.74 (s, 1H), 7.48 (s, 4H), 6.08 (s, 1H), 5.85 (d, $J = 9.3$ Hz, 1H), 5.81 (s, 1H), 5.40 (t, $J = 9.3$ Hz, 1H), 5.34 (t, $J = 10.0$ Hz, 1H), 5.20 (t, $J = 10.0$ Hz, 1H), 5.11–5.03 (m, 2H), 4.27 (dd, $J = 12.7, 5.5$ Hz, 1H), 4.13 (dd, $J = 12.0$ Hz, 2.5 Hz, 1H), 4.02–3.99 (m, 1H), 2.04 (s, 6H), 2.00 (s, 3H), 1.79 (s, 3H). ^{13}C NMR (125 MHz, CDCl_3) δ 170.4, 169.8, 169.4, 169.0, 155.9, 152.4, 143.6, 143.2, 142.2, 137.1, 130.8, 130.3, 129.5, 121.0, 100.3, 91.0, 85.9, 75.4, 72.3, 70.5, 67.7, 61.5, 45.8, 20.7, 20.5, 20.5, 20.1. HRMS (ESI-TOF), m/z calcd. $\text{C}_{29}\text{H}_{30}\text{ClN}_6\text{O}_{10}$ $[\text{M} + \text{H}]^+$ 657.1706; found: 657.2048.

4.2.5 (2S,3S,4R,5S,6S)-2-(Acetoxymethyl)-6-(4-((5-(4-fluorophenyl)-7-oxopyrazolo[1,5-*a*]pyrimidin-1(7*H*)-yl)methyl)-1*H*-1,2,3-triazol-1-yl)tetrahydro-2*H*-pyran-3,4,5-triyl triacetate (26). Light yellow colored sticky solid; yield: 132.74 mg (95%), $R_f = 0.20$ (ethyl acetate); ^1H NMR (500 MHz, CDCl_3) δ 7.81 (s, 1H), 7.75 (s, 1H), 7.52 (dd, $J = 9.1, 5.1$ Hz, 2H), 7.18 (d, $J = 8.2$ Hz, 2H), 6.07 (s, 1H), 5.86 (d, $J = 9.1$ Hz, 1H), 5.80 (s, 1H), 5.40 (t, $J = 9.5$ Hz, 1H), 5.34 (t, $J = 9.0$ Hz, 1H), 5.19 (t, $J = 9.5$ Hz, 1H), 5.10–5.03 (m, 2H), 4.27 (dd, $J = 12.7, 5.0$ Hz, 1H), 4.12 (dd, $J = 12.5$ Hz, 2.5 Hz, 1H), 4.02–3.99 (m, 1H), 2.03 (s, 6H), 1.99 (s, 3H), 1.78 (s, 3H). ^{13}C NMR (125 MHz, CDCl_3) δ 170.4, 169.8, 169.4, 169., 164.9, 162.9, 155.9, 152.6, 143.5, 143.2, 142.3, 131.0, 131.0, 128.5, 121.1, 116.5, 116.3, 100.3, 91.0, 85.9, 75.3, 72.3, 70.5, 67.7, 61.5, 45.7, 20.7, 20.5, 20.5, 20.1. ^{13}C – ^{19}F couplings in ^{13}C NMR: (125 MHz, CDCl_3) δ 163.9 (d, $J_{\text{C-F}} = 253.26$ Hz, C_1), 131.0 (d, $J_{\text{C-F}} = 7.56$ Hz, C_3), 116.4 (d, $J_{\text{C-F}} = 22.68$ Hz, C_2). HRMS (ESI-TOF), m/z calcd. $\text{C}_{29}\text{H}_{30}\text{FN}_6\text{O}_{10}$ $[\text{M} + \text{H}]^+$ 641.2002; found: 641.2324.

4.2.6 (2S,3S,4R,5S,6S)-2-(Acetoxymethyl)-6-(4-((7-oxo-5-(4-(trifluoromethyl)phenyl)pyrazolo[1,5-*a*]pyrimidin-1(7*H*)-yl)methyl)-1*H*-1,2,3-triazol-1-yl)tetrahydro-2*H*-pyran-3,4,5-triyl

triacetate (27). Light brown colored sticky solid; yield: 117.47 mg (95%), $R_f = 0.20$ (ethyl acetate); ^1H NMR (500 MHz, CDCl_3) δ 7.84 (s, 1H), 7.78 (d, $J = 6.7$ Hz, 3H), 7.71 (d, $J = 8.0$ Hz, 2H), 6.08 (s, 1H), 5.85 (d, $J = 9.5$ Hz, 1H), 5.82 (s, 1H), 5.40 (t, $J = 9.5$ Hz, 1H), 5.34 (t, $J = 9.0$ Hz, 1H), 5.19 (t, $J = 9.5$ Hz, 1H), 5.05 (s, 2H), 4.27 (dd, $J = 12.0, 5.5$ Hz, 1H), 4.13 (dd, $J = 13.3$ Hz, 2.5 Hz, 1H), 4.02–3.99 (m, 1H), 2.04 (s, 3H), 2.03 (s, 3H), 2.00 (s, 3H), 1.79 (s, 3H). ^{13}C NMR (125 MHz, CDCl_3) δ 170.5, 169.8, 169.4, 169.1, 155.8, 152.0, 143.7, 143.1, 142.0, 136.0, 132.9, 132.7, 132.4, 129.5, 126.8, 126.2, 124, 122.5, 121.1, 100.5, 91.1, 86.0, 72.3, 70.5, 67.8, 61.5, 45.9, 20.7, 20.6, 20.5, 20.1. ^{13}C – ^{19}F couplings in ^{13}C NMR: (125 MHz, CDCl_3) δ 132.8 (q, $J_{\text{C-F}} = 32.76$ Hz, C_2), 126.2 (d, $J_{\text{C-F}} = 3.78$ Hz, C_3), 123.6 (q, $J_{\text{C-F}} = 273.42$ Hz, C_1). HRMS (ESI-TOF), m/z calcd. $\text{C}_{30}\text{H}_{30}\text{F}_3\text{N}_6\text{O}_{10}$ $[\text{M} + \text{H}]^+$ 691.1970; found: 691.2329.

4.2.7 (2S,3S,4R,5S,6S)-2-(Acetoxymethyl)-6-(4-((5-(4-iso-propylphenyl)-7-oxopyrazolo[1,5-*a*]pyrimidin-1(7*H*)-yl)methyl)-1*H*-1,2,3-triazol-1-yl)tetrahydro-2*H*-pyran-3,4,5-triyl triacetate (28). Off white colored sticky solid; yield: 122.53 mg (96%), $R_f = 0.22$ (ethyl acetate); ^1H NMR (500 MHz, CDCl_3) δ 7.82 (s, 1H), 7.64 (s, 1H), 7.41 (d, $J = 8.0$ Hz, 2H), 7.35 (d, $J = 8.0$ Hz, 2H), 6.07 (s, 1H), 5.85 (s, 1H), 5.84 (d, $J = 9.5$ Hz, 1H), 5.40 (t, $J = 9.0$ Hz, 1H), 5.34 (t, $J = 9.0$ Hz, 1H), 5.20 (t, $J = 10.0$ Hz, 1H), 5.16–5.08 (m, 2H), 4.28 (dd, $J = 12.0, 5.5$ Hz, 1H), 4.12 (dd, $J = 12.0$ Hz, 2.5 Hz, 1H), 4.01–3.98 (m, 1H), 2.97 (hept, $J = 6.7$ Hz, 1H), 2.04 (s, 6H), 2.00 (s, 3H), 1.77 (s, 3H), 1.28 (d, $J = 6.7$ Hz, 6H). ^{13}C NMR (125 MHz, CDCl_3) δ 170.5, 169.8, 169.4, 168.9, 156.2, 153.7, 151.8, 143.5, 143.2, 142.6, 129.9, 128.7, 127.3, 120.9, 100.2, 90.9, 85.9, 75.4, 72.4, 70.4, 67.7, 61.5, 45.7, 34.1, 23.9, 23.8, 20.7, 20.5, 20.1. HRMS (ESI-TOF), m/z calcd. $\text{C}_{32}\text{H}_{37}\text{N}_6\text{O}_{10}$ $[\text{M} + \text{H}]^+$ 665.2566; found: 665.2909.

4.2.8 (2S,3S,4R,5S,6S)-2-(Acetoxymethyl)-6-(4-((5-(naphthalen-2-yl)-7-oxopyrazolo[1,5-*a*]pyrimidin-1(7*H*)-yl)methyl)-1*H*-1,2,3-triazol-1-yl)tetrahydro-2*H*-pyran-3,4,5-triyl triacetate (29). Light brown colored sticky solid; yield: 124.85 mg (97%), $R_f = 0.23$ (ethyl acetate); ^1H NMR (500 MHz, CDCl_3) δ 8.04 (s, 1H), 7.97 (d, $J = 8.0$ Hz, 1H), 7.92 (t, $J = 8.0$ Hz, 2H), 7.86 (s, 1H), 7.64 (s, 1H), 7.62–7.52 (m, 3H), 6.14 (s, 1H), 5.96 (s, 1H), 5.84 (d, $J = 9.3$ Hz, 1H), 5.40 (t, $J = 9.5$ Hz, 1H), 5.33 (t, $J = 9.0$ Hz, 1H), 5.21–5.10 (m, 3H), 4.26 (dd, $J = 13.5, 4.0$ Hz, 1H), 4.12 (dd, $J = 12.0$ Hz, 2.0 Hz, 1H), 4.01–3.98 (m, 1H), 2.04 (s, 3H), 2.03 (s, 3H), 2.01 (s, 3H), 1.77 (s, 3H). ^{13}C NMR (125 MHz, CDCl_3) δ 170.4, 169.8, 169.4, 168.9, 156.1, 153.6, 143.6, 143.3, 142.4, 133.9, 132.8, 129.8, 129.1, 129.0, 128.6, 128.0, 127.5, 125.2, 121.1, 100.5, 91.0, 85.9, 75.3, 72.4, 70.4, 67.8, 61.5, 45.8, 20.7, 20.6, 20.5, 20.1. HRMS (ESI-TOF), m/z calcd. $\text{C}_{33}\text{H}_{33}\text{N}_6\text{O}_{10}$ $[\text{M} + \text{H}]^+$ 673.2253; found: 673.2591.

4.2.9 (2S,3S,4R,5S,6S)-2-(Acetoxymethyl)-6-(4-((5-(benzo[d][1,3]dioxol-5-yl)-7-oxopyrazolo[1,5-*a*]pyrimidin-1(7*H*)-yl)methyl)-1*H*-1,2,3-triazol-1-yl)tetrahydro-2*H*-pyran-3,4,5-triyl triacetate (30). Yellow colored sticky solid; yield: 127.96 mg (98%), $R_f = 0.21$ (ethyl acetate); ^1H NMR (500 MHz, CDCl_3) δ 7.82 (s, 1H), 7.69 (s, 1H), 6.97 (s, 1H), 6.95 (s, 1H), 6.90 (d, $J = 8.3$ Hz, 1H), 6.06 (s, 1H), 6.04 (s, 2H), 5.84 (d, $J = 9.3$ Hz, 1H), 5.83 (s, 1H), 5.40 (t, $J = 9.0$ Hz, 1H), 5.34 (t, $J = 9.0$ Hz, 1H), 5.22–5.08 (m, 3H), 4.27 (dd, $J = 13.0, 5.0$ Hz, 1H), 4.12 (dd, $J = 12.0$



Hz, 2.0 Hz, 1H), 4.01–3.98 (m, 1H), 2.04 (s, 6H), 2.00 (s, 3H), 1.78 (s, 3H). ^{13}C NMR (125 MHz, CDCl_3) δ 170.5, 169.8, 169.4, 169.0, 156.1, 153.2, 149.6, 148.3, 143.5, 143.2, 142.5, 125.9, 123.2, 121.0, 109.0, 108.9, 101.9, 100.2, 90.9, 85.9, 75.3, 72.3, 70.4, 67.7, 61.5, 45.7, 20.7, 20.6, 20.5, 20.1. HRMS (ESI-TOF), m/z calcd. $\text{C}_{30}\text{H}_{31}\text{N}_6\text{O}_{12}$ $[\text{M} + \text{H}]^+$ 667.1994; found: 667.2330.

4.2.10 (2*S*,3*R*,4*R*,5*S*,6*S*)-2-(Acetoxymethyl)-6-(4-((7-oxo-5-(*p*-tolyl)pyrazolo[1,5-*a*]pyrimidin-1(7*H*)-yl)methyl)-1*H*-1,2,3-triazol-1-yl)tetrahydro-2*H*-pyran-3,4,5-triyl triacetate (31). Light yellow colored powder; yield: 118.53 mg (98%), R_f = 0.22 (ethyl acetate); ^1H NMR (500 MHz, CDCl_3) δ 7.84 (s, 1H), 7.63 (s, 1H), 7.37 (d, J = 8.0 Hz, 2H), 7.29 (d, J = 8.0 Hz, 2H), 6.07 (s, 1H), 5.85 (s, 1H), 5.82 (d, J = 9.3 Hz, 1H), 5.52 (d, J = 4.0 Hz, 1H), 5.43 (t, J = 9.5 Hz, 1H), 5.25 (t, J = 11.0 Hz, 1H), 5.16–5.07 (m, 2H), 4.25–2.22 (m, 1H), 4.18–4.08 (m, 2H), 2.41 (s, 3H), 2.19 (s, 3H), 2.01 (s, 3H), 1.98 (s, 3H), 1.80 (s, 3H). ^{13}C NMR (125 MHz, CDCl_3) δ 170.35, 169.9, 169.7, 169.1, 156.2, 153.8, 143.5, 143.3, 142.6, 141.0, 129.8, 129.6, 128.6, 120.8, 100.1, 90.9, 86.4, 74.3, 70.5, 68.0, 66.8, 61.1, 45.8, 21.5, 20.7, 20.6, 20.5, 20.2. HRMS (ESI-TOF), m/z calcd. $\text{C}_{30}\text{H}_{33}\text{N}_6\text{O}_{10}$ $[\text{M} + \text{H}]^+$ 637.2253; found: 637.2571.

4.2.11 (2*S*,3*R*,4*R*,5*S*,6*S*)-2-(Acetoxymethyl)-6-(4-((5-(4-methoxyphenyl)-7-oxopyrazolo[1,5-*a*]pyrimidin-1(7*H*)-yl)methyl)-1*H*-1,2,3-triazol-1-yl)tetrahydro-2*H*-pyran-3,4,5-triyl triacetate (32). Off white colored powder; yield: 113.32 mg (97%), R_f = 0.21 (ethyl acetate); ^1H NMR (500 MHz, CDCl_3) δ 7.83 (s, 1H), 7.64 (s, 1H), 7.42 (d, J = 8.1 Hz, 2H), 6.99 (d, J = 8.2 Hz, 2H), 6.06 (s, 1H), 5.84 (s, 1H), 5.82 (d, J = 11.0 Hz, 1H), 5.52 (d, J = 3.5 Hz, 1H), 5.43 (t, J = 9.5 Hz, 1H), 5.23 (dd, J = 10.0 Hz, 3.5 Hz, 1H), 5.17–5.07 (m, 2H), 4.24 (t, J = 6.1 Hz, 1H), 4.17–4.07 (m, 2H), 3.84 (s, 3H), 2.19 (s, 3H), 2.00 (s, 3H), 1.97 (s, 3H), 1.80 (s, 3H). ^{13}C NMR (125 MHz, CDCl_3) δ 170.3, 169.9, 169.7, 169.1, 161.4, 156.2, 153.6, 143.5, 143.4, 142.6, 130.3, 124.6, 120.8, 114.6, 100.1, 90.9, 86.4, 74.3, 70.5, 68.0, 66.8, 61.1, 55.5, 45.9, 20.7, 20.6, 20.5, 20.2. HRMS (ESI-TOF), m/z calcd. $\text{C}_{30}\text{H}_{33}\text{N}_6\text{O}_{11}$ $[\text{M} + \text{H}]^+$ 653.2202; found: 653.2535.

4.2.12 (2*S*,3*R*,4*R*,5*S*,6*S*)-2-(Acetoxymethyl)-6-(4-((5-(4-bromophenyl)-7-oxopyrazolo[1,5-*a*]pyrimidin-1(7*H*)-yl)methyl)-1*H*-1,2,3-triazol-1-yl)tetrahydro-2*H*-pyran-3,4,5-triyl triacetate (33). Yellow colored crystalline solid; yield: 101.64 mg (98%), R_f = 0.23 (ethyl acetate); ^1H NMR (500 MHz, CDCl_3) δ 7.83 (s, 1H), 7.69 (s, 1H), 7.63 (d, J = 9.3 Hz, 2H), 7.41 (d, J = 9.3 Hz, 2H), 6.07 (s, 1H), 5.82 (d, J = 9.0 Hz, 1H), 5.80 (s, 1H), 5.52 (d, J = 4.0 Hz, 1H), 5.42 (t, J = 10.0 Hz, 1H), 5.24 (dd, J = 10.5 Hz, 4.0 Hz, 1H), 5.10–5.03 (m, 2H), 4.24 (t, J = 7.0 Hz, 1H), 4.17–4.10 (m, 2H), 2.18 (s, 3H), 2.00 (s, 3H), 1.98 (s, 3H), 1.80 (s, 3H). ^{13}C NMR (125 MHz, CDCl_3) δ 170.3, 169.9, 169.7, 169.2, 155.9, 152.4, 143.6, 143.2, 142.2, 132.4, 131.3, 130.5, 125.3, 120.9, 100.2, 91.0, 86.4, 74.3, 70.5, 68.1, 66.8, 61.1, 45.9, 20.7, 20.6, 20.5, 20.2. HRMS (ESI-TOF), m/z calcd. $\text{C}_{29}\text{H}_{30}\text{BrN}_6\text{O}_{10}$ $[\text{M} + \text{H}]^+$ 701.1201; found: 701.1589.

4.2.13 (2*S*,3*R*,4*R*,5*S*,6*S*)-2-(Acetoxymethyl)-6-(4-((5-(4-chlorophenyl)-7-oxopyrazolo[1,5-*a*]pyrimidin-1(7*H*)-yl)methyl)-1*H*-1,2,3-triazol-1-yl)tetrahydro-2*H*-pyran-3,4,5-triyl triacetate (34). Light yellow colored sticky solid; yield: 117.61 mg (98%), R_f = 0.23 (ethyl acetate); ^1H NMR (500 MHz, CDCl_3) δ 7.84 (s, 1H), 7.68 (s, 1H), 7.47 (s, 4H), 6.08 (s, 1H), 5.82 (d, J = 9.0 Hz, 1H),

5.81 (s, 1H), 5.53 (d, J = 4.0 Hz, 1H), 5.41 (t, J = 10.0 Hz, 1H), 5.24 (dd, J = 9.5 Hz, 4.0 Hz, 1H), 5.11–5.03 (m, 2H), 4.24 (t, J = 6.5 Hz, 1H), 4.17–4.13 (m, 2H), 2.18 (s, 3H), 2.01 (s, 3H), 1.98 (s, 3H), 1.81 (s, 3H). ^{13}C NMR (125 MHz, CDCl_3) δ 170.3, 169.9, 169.7, 169.2, 155.9, 152.4, 143.6, 143.3, 142.2, 137.1, 130.8, 130.3, 129.5, 120.9, 100.3, 91.0, 86.4, 74.3, 70.5, 68.1, 66.8, 61.1, 45.9, 20.7, 20.5, 20.2. HRMS (ESI-TOF), m/z calcd. $\text{C}_{29}\text{H}_{30}\text{ClN}_6\text{O}_{10}$ $[\text{M} + \text{H}]^+$ 657.1706; found: 657.2042.

4.2.14 (2*S*,3*R*,4*R*,5*S*,6*S*)-2-(Acetoxymethyl)-6-(4-((5-(4-fluorophenyl)-7-oxopyrazolo[1,5-*a*]pyrimidin-1(7*H*)-yl)methyl)-1*H*-1,2,3-triazol-1-yl)tetrahydro-2*H*-pyran-3,4,5-triyl triacetate (35). Light yellow colored crystalline solid; yield: 132.74 mg (95%), R_f = 0.20 (ethyl acetate); ^1H NMR (500 MHz, CDCl_3) δ 7.82 (s, 1H), 7.68 (s, 1H), 7.52 (dd, J = 8.7, 4.7 Hz, 2H), 7.17 (d, J = 8.7 Hz, 2H), 6.07 (s, 1H), 5.83 (d, J = 9.3 Hz, 1H), 5.80 (s, 1H), 5.51 (d, J = 4.0 Hz, 1H), 5.42 (t, J = 10.0 Hz, 1H), 5.24 (dd, J = 9.3, 4.0 Hz, 1H), 5.12–5.02 (m, 2H), 4.24 (t, J = 6.0 Hz, 1H), 4.17–4.09 (m, 2H), 2.17 (s, 3H), 1.99 (s, 3H), 1.97 (s, 3H), 1.79 (s, 3H). ^{13}C NMR (125 MHz, CDCl_3) δ 170.3, 169.9, 169.7, 169.2, 164.9, 162.9, 155.9, 152.6, 143.6, 143.3, 142.2, 131.1, 131.0, 128.5, 120.9, 116.4, 116.3, 100.3, 90.9, 86.3, 74.3, 70.5, 68.0, 66.8, 61.1, 45.8, 20.6, 20.5, 20.2. ^{13}C – ^{19}F couplings in ^{13}C NMR: (125 MHz, CDCl_3) δ 163.9 (d, $J_{\text{C-F}}$ = 252.0 Hz, C_1), 131.0 (d, $J_{\text{C-F}}$ = 7.56 Hz, C_3), 116.3 (d, $J_{\text{C-F}}$ = 22.68 Hz, C_2). HRMS (ESI-TOF), m/z calcd. $\text{C}_{29}\text{H}_{30}\text{FN}_6\text{O}_{10}$ $[\text{M} + \text{H}]^+$ 641.2002; found: 641.2320.

4.2.15 (2*S*,3*R*,4*R*,5*S*,6*S*)-2-(Acetoxymethyl)-6-(4-((7-oxo-5-(4-(trifluoromethyl)phenyl)pyrazolo[1,5-*a*]pyrimidin-1(7*H*)-yl)methyl)-1*H*-1,2,3-triazol-1-yl)tetrahydro-2*H*-pyran-3,4,5-triyl triacetate (36). Yellow colored crystalline solid; yield: 116.24 mg (94%), R_f = 0.20 (ethyl acetate); ^1H NMR (500 MHz, CDCl_3) δ 7.86 (s, 1H), 7.78 (d, J = 8.0 Hz, 2H), 7.70 (d, J = 6.1 Hz, 3H), 6.10 (s, 1H), 5.83 (s, 1H), 5.82 (d, J = 9.5 Hz, 1H), 5.53 (d, J = 4.0 Hz, 1H), 5.42 (t, J = 10.0 Hz, 1H), 5.25 (dd, J = 9.5 Hz, 3.5 Hz, 1H), 5.06 (br s, 2H), 4.24 (t, J = 6.5 Hz, 1H), 4.16–4.12 (m, 2H), 2.18 (s, 3H), 2.01 (s, 3H), 1.99 (s, 3H), 1.81 (s, 3H). ^{13}C NMR (125 MHz, CDCl_3) δ 170.3, 169.9, 169.7, 169.3, 155.8, 152.0, 143.7, 143.2, 142.0, 135.9, 132.9, 132.6, 132.4, 129.6, 126.2, 124.7, 122.5, 120.9, 100.4, 91.1, 86.5, 70.5, 68.1, 66.8, 61.1, 45.9, 20.6, 20.5, 20.3. ^{13}C – ^{19}F couplings in ^{13}C NMR: (125 MHz, CDCl_3) δ 132.8 (q, $J_{\text{C-F}}$ = 32.76 Hz, C_2), 126.2 (d, $J_{\text{C-F}}$ = 3.78 Hz, C_3), 123.6 (q, $J_{\text{C-F}}$ = 272.16 Hz, C_1). HRMS (ESI-TOF), m/z calcd. $\text{C}_{30}\text{H}_{30}\text{F}_3\text{N}_6\text{O}_{10}$ $[\text{M} + \text{H}]^+$ 691.1970; found: 691.2330.

4.2.16 (2*S*,3*R*,4*R*,5*S*,6*S*)-2-(Acetoxymethyl)-6-(4-((5-(4-isopropylphenyl)-7-oxopyrazolo[1,5-*a*]pyrimidin-1(7*H*)-yl)methyl)-1*H*-1,2,3-triazol-1-yl)tetrahydro-2*H*-pyran-3,4,5-triyl triacetate (37). Yellow colored crystalline solid; yield: 122.53 mg (96%), R_f = 0.23 (ethyl acetate); ^1H NMR (500 MHz, CDCl_3) δ 7.84 (s, 1H), 7.64 (s, 1H), 7.41 (d, J = 7.9 Hz, 2H), 7.33 (d, J = 8.0 Hz, 2H), 6.06 (s, 1H), 5.86 (s, 1H), 5.82 (d, J = 9.3 Hz, 1H), 5.52 (d, J = 3.6 Hz, 1H), 5.44 (t, J = 9.9 Hz, 1H), 5.24 (dd, J = 10.0, 4.7 Hz, 1H), 5.17–5.07 (m, 2H), 4.24 (t, J = 6.0 Hz, 1H), 4.18–4.10 (m, 2H), 2.96 (hept, J = 6.7 Hz, 1H), 2.18 (s, 3H), 2.00 (s, 3H), 1.98 (s, 3H), 1.80 (s, 3H), 1.27 (d, J = 6.7 Hz, 6H). ^{13}C NMR (125 MHz, CDCl_3) δ 170.3, 169.9, 169.7, 169.1, 156.2, 153.8, 151.8, 143.5, 143.3, 142.6, 129.9, 128.7, 127.2, 120.8, 100.1, 90.9, 86.4, 74.3, 70.5, 67.9, 66.8, 61.1, 45.9, 34.1, 23.8, 20.7, 20.7, 20.5, 20.2. HRMS



(ESI-TOF), m/z calcd. $C_{32}H_{37}N_6O_{10}$ $[M + H]^+$ 665.2566; found: 665.2905.

4.2.17 (2S,3R,4R,5S,6S)-2-(Acetoxymethyl)-6-(4-((5-(naphthalen-2-yl)-7-oxopyrazolo[1,5-a]pyrimidin-1(7H)-yl)methyl)-1H-1,2,3-triazol-1-yl)tetrahydro-2H-pyran-3,4,5-triyl triacetate (38). Yellow colored sticky solid; yield: 124.85 mg (97%), R_f = 0.23 (ethyl acetate); 1H NMR (500 MHz, $CDCl_3$) δ 8.04 (s, 1H), 7.97–7.88 (m, 3H), 7.86 (s, 1H), 7.65 (s, 1H), 7.58 (dt, J = 13.3, 6.7 Hz, 3H), 6.14 (s, 1H), 5.94 (s, 1H), 5.83 (d, J = 9.3 Hz, 1H), 5.52 (d, J = 5.3 Hz, 1H), 5.43 (t, J = 10.0 Hz, 1H), 5.25 (dd, J = 10.7, 4.0 Hz, 1H), 5.19–5.09 (m, 2H), 4.24 (t, J = 6.0 Hz, 1H), 4.17–4.10 (m, 2H), 2.17 (s, 3H), 2.00 (s, 3H), 1.98 (s, 3H), 1.78 (s, 3H). ^{13}C NMR (125 MHz, $CDCl_3$) δ 170.3, 169.9, 169.7, 169.1, 156.1, 153.6, 143.6, 143.3, 142.3, 133.8, 132.8, 129.8, 129.1, 129.0, 128.5, 127.9, 127.9, 127.4, 125.2, 121.0, 100.4, 91.0, 86.3, 74.2, 70.5, 68.0, 66.8, 61.1, 45.8, 20.6, 20.5, 20.2. HRMS (ESI-TOF), m/z calcd. $C_{33}H_{33}N_6O_{10}$ $[M + H]^+$ 673.2253; found: 673.2583.

4.2.18 (2S,3R,4R,5S,6S)-2-(Acetoxymethyl)-6-(4-((5-(benzo[d][1,3]dioxol-5-yl)-7-oxopyrazolo[1,5-a]pyrimidin-1(7H)-yl)methyl)-1H-1,2,3-triazol-1-yl)tetrahydro-2H-pyran-3,4,5-triyl triacetate (39). Yellow colored crystalline solid; yield: 126.66 mg (97%), R_f = 0.21 (ethyl acetate); 1H NMR (500 MHz, $CDCl_3$) δ 7.83 (s, 1H), 7.67 (s, 1H), 6.96 (d, J = 8.0 Hz, 2H), 6.88 (d, J = 8.0 Hz, 1H), 6.05 (s, 1H), 6.03 (s, 2H), 5.82 (s, 1H), 5.81 (d, J = 8.0 Hz, 1H), 5.51 (d, J = 5.5 Hz, 1H), 5.42 (t, J = 10.0 Hz, 1H), 5.24 (dd, J = 10.0 Hz, 4.5 Hz, 1H), 5.19–5.07 (m, 2H), 4.24 (t, J = 6.5 Hz, 1H), 4.17–4.10 (m, 2H), 2.17 (s, 3H), 2.00 (s, 3H), 1.97 (s, 3H), 1.79 (s, 3H). ^{13}C NMR (125 MHz, $CDCl_3$) δ 170.34, 169.9, 169.7, 169.2, 156.1, 153.2, 149.6, 148.2, 143.5, 143.2, 142.5, 125.8, 123.2, 120.8, 109.0, 108.9, 101.9, 100.1, 90.9, 86.4, 74.2, 70.5, 67.9, 66.8, 61.1, 45.8, 20.7, 20.6, 20.5, 20.1. HRMS (ESI-TOF), m/z calcd. $C_{30}H_{31}N_6O_{12}$ $[M + H]^+$ 667.1994; found: 667.2314.

4.2.19 (2R,3R,4S,5S,6S)-2-(Acetoxymethyl)-6-(4-((7-oxo-5-(p-tolyl)pyrazolo[1,5-a]pyrimidin-1(7H)-yl)methyl)-1H-1,2,3-triazol-1-yl)tetrahydro-2H-pyran-3,4,5-triyl triacetate (40). Yellow colored sticky solid; yield: 114.90 mg (95%), R_f = 0.21 (ethyl acetate); 1H NMR (500 MHz, $CDCl_3$) δ 7.76 (s, 2H), 7.36 (d, J = 7.8 Hz, 2H), 7.30 (d, J = 7.7 Hz, 2H), 6.11 (s, 1H), 6.03 (br s, 1H), 5.85 (t, J = 4.0 Hz, 1H), 5.82 (dd, J = 9.0 Hz, 3.5 Hz, 1H), 5.77 (s, 1H), 5.30 (t, J = 9.0 Hz, 1H), 5.16 (br s, 2H), 4.34 (dd, J = 12.5, 5.5 Hz, 1H), 4.00 (dd, J = 12.0 Hz, 2.5 Hz, 1H), 3.88–3.85 (m, 1H), 2.41 (s, 3H), 2.11 (s, 3H), 2.04 (s, 3H), 2.02 (s, 6H). ^{13}C NMR (125 MHz, $CDCl_3$) δ 170.5, 169.6, 169.4, 156.1, 153.6, 142.3, 141.1, 129.9, 129.5, 128.6, 123.3, 100.0, 83.5, 77.4, 77.3, 77.1, 76.9, 72.5, 68.7, 68.1, 66.1, 61.5, 45.5, 21.5, 20.7, 20.6. HRMS (ESI-TOF), m/z calcd. $C_{30}H_{33}N_6O_{10}$ $[M + H]^+$ 637.2253; found: 637.2560.

4.2.20 (2R,3R,4S,5S,6S)-2-(Acetoxymethyl)-6-(4-((5-(4-methoxyphenyl)-7-oxopyrazolo[1,5-a]pyrimidin-1(7H)-yl)methyl)-1H-1,2,3-triazol-1-yl)tetrahydro-2H-pyran-3,4,5-triyl triacetate (41). Light yellow colored crystalline solid; yield: 112.16 mg (96%), R_f = 0.22 (ethyl acetate); 1H NMR (500 MHz, $CDCl_3$) δ 7.82 (s, 1H), 7.63 (s, 1H), 7.42 (d, J = 8.2 Hz, 2H), 7.03 (d, J = 7.9 Hz, 2H), 6.12 (s, 1H), 6.00 (s, 1H), 5.88 (t, J = 4.0 Hz, 1H), 5.83 (s, 1H), 5.82 (dd, J = 9.0 Hz, 3.5 Hz, 1H), 5.31 (t, J = 8.5 Hz, 1H), 5.18 (br s, 2H), 4.38 (dd, J = 12.5, 5.5 Hz, 1H), 4.03 (dd, J = 13.5 Hz, 2.5 Hz, 1H), 3.87–3.85 (m, 4H), 2.13 (s, 3H), 2.06 (s, 3H), 2.05 (s, 3H), 2.04 (s, 3H). ^{13}C NMR (125 MHz, $CDCl_3$)

δ 170.6, 169.7, 169.4, 161.4, 156.1, 153.4, 143.5, 143.3, 142.5, 130.3, 124.5, 122.9, 114.7, 100.3, 90.8, 83.5, 72.7, 68.7, 68.1, 66.2, 61.5, 55.6, 45.5, 20.8, 20.7. HRMS (ESI-TOF), m/z calcd. $C_{30}H_{33}N_6O_{11}$ $[M + H]^+$ 653.2202; found: 653.2540.

4.2.21 (2R,3R,4S,5S,6S)-2-(Acetoxymethyl)-6-(4-((5-(4-bromophenyl)-7-oxopyrazolo[1,5-a]pyrimidin-1(7H)-yl)methyl)-1H-1,2,3-triazol-1-yl)tetrahydro-2H-pyran-3,4,5-triyl triacetate (42). Off-white colored powder; yield: 98.53 mg (95%), R_f = 0.23 (ethyl acetate); 1H NMR (500 MHz, $CDCl_3$) δ 7.88 (s, 1H), 7.73 (s, 1H), 7.66 (d, J = 8.0 Hz, 2H), 7.44 (d, J = 8.2 Hz, 2H), 6.08 (s, 1H), 6.05 (br s, 1H), 5.85 (t, J = 4.0 Hz, 1H), 5.80 (dd, J = 8.5 Hz, 3.5 Hz, 1H), 5.74 (s, 1H), 5.31 (t, J = 9.5 Hz, 1H), 5.11 (br s, 2H), 4.35 (dd, J = 12.0, 5.5 Hz, 1H), 4.01 (dd, J = 12.0 Hz, 2.5 Hz, 1H), 3.90–3.87 (m, 1H), 2.11 (s, 3H), 2.04 (s, 3H), 2.03 (s, 6H). ^{13}C NMR (125 MHz, $CDCl_3$) δ 170.5, 169.6, 169.5, 155.8, 152.4, 143.5, 143.0, 141.8, 132.5, 131.3, 130.5, 125.4, 123.4, 100.2, 90.9, 83.5, 72.6, 68.7, 68.1, 66.1, 61.5, 45.5, 20.7, 20.6. HRMS (ESI-TOF), m/z calcd. $C_{29}H_{30}BrN_6O_{10}$ $[M + H]^+$ 701.1201; found: 701.1588.

4.2.22 (2R,3R,4S,5S,6S)-2-(Acetoxymethyl)-6-(4-((5-(4-chlorophenyl)-7-oxopyrazolo[1,5-a]pyrimidin-1(7H)-yl)methyl)-1H-1,2,3-triazol-1-yl)tetrahydro-2H-pyran-3,4,5-triyl triacetate (43). Light yellow colored sticky solid; yield: 115.21 mg (96%), R_f = 0.23 (ethyl acetate); 1H NMR (500 MHz, $CDCl_3$) δ 7.80 (s, 1H), 7.77 (s, 1H), 7.51 (s, 4H), 6.12 (s, 1H), 6.04 (s, 1H), 5.85 (t, J = 4.0 Hz, 1H), 5.80 (dd, J = 8.5 Hz, 3.5 Hz, 1H), 5.79 (s, 1H), 5.31 (t, J = 8.0 Hz, 1H), 5.12 (br s, 2H), 4.38 (dd, J = 12.5, 5.5 Hz, 1H), 4.03 (dd, J = 12.0 Hz, 2.5 Hz, 1H), 3.90–3.87 (m, 1H), 2.12 (s, 3H), 2.06 (s, 3H), 2.04 (s, 6H). ^{13}C NMR (125 MHz, $CDCl_3$) δ 170.6, 169.7, 169.5, 155.9, 152.3, 141.9, 137.2, 130.8, 130.3, 129.6, 123.1, 100.4, 83.5, 72.8, 68.7, 68.1, 66.2, 61.5, 45.5, 20.8, 20.7. HRMS (ESI-TOF), m/z calcd. $C_{29}H_{30}ClN_6O_{10}$ $[M + H]^+$ 657.1706; found: 657.2059.

4.2.23 (2R,3R,4S,5S,6S)-2-(Acetoxymethyl)-6-(4-((5-(4-fluorophenyl)-7-oxopyrazolo[1,5-a]pyrimidin-1(7H)-yl)methyl)-1H-1,2,3-triazol-1-yl)tetrahydro-2H-pyran-3,4,5-triyl triacetate (44). Off-white colored sticky solid; yield: 125.75 mg (90%), R_f = 0.20 (ethyl acetate); 1H NMR (500 MHz, $CDCl_3$) δ 7.90 (s, 1H), 7.76 (s, 1H), 7.55 (dd, J = 6.5 Hz, 2H), 7.21 (d, J = 8.5 Hz, 2H), 6.11 (s, 1H), 6.06 (s, 1H), 5.85 (br s, 1H), 5.81 (dd, J = 8.5 Hz, 3.5 Hz, 1H), 5.74 (s, 1H), 5.31 (t, J = 8.6 Hz, 1H), 5.12 (br s, 2H), 4.34 (dd, J = 12.5, 5.5 Hz, 1H), 4.01 (dd, J = 12.5 Hz, 2.5 Hz, 1H), 3.90–3.87 (m, 1H), 2.10 (s, 3H), 2.04 (s, 3H), 2.02 (s, 6H). ^{13}C NMR (125 MHz, $CDCl_3$) δ 170.5, 169.6, 169.4, 164.9, 162.9, 155.9, 152.5, 141.9, 131.1, 131.0, 128.5, 123.5, 116.6, 116.4, 100.3, 83.6, 72.6, 68.7, 68.1, 66.1, 61.6, 45.6, 20.7, 20.6. ^{13}C – ^{19}F couplings in ^{13}C NMR: (125 MHz, $CDCl_3$) δ 163.9 (d, J_{C-F} = 253.26 Hz, C_1), 131.0 (d, J_{C-F} = 8.82 Hz, C_3), 116.5 (d, J_{C-F} = 23.94 Hz, C_2). HRMS (ESI-TOF), m/z calcd. $C_{29}H_{30}FN_6O_{10}$ $[M + H]^+$ 641.2002; found: 641.2321.

4.2.24 (2R,3R,4S,5S,6S)-2-(Acetoxymethyl)-6-(4-((7-oxo-5-(4-(trifluoromethyl)phenyl)pyrazolo[1,5-a]pyrimidin-1(7H)-yl)methyl)-1H-1,2,3-triazol-1-yl)tetrahydro-2H-pyran-3,4,5-triyl triacetate (45). Off-white colored powder; yield: 111.29 mg (90%), R_f = 0.20 (ethyl acetate); 1H NMR (500 MHz, $CDCl_3$) δ 7.85 (s, 1H), 7.81 (d, J = 8.0 Hz, 3H), 7.74 (d, J = 8.1 Hz, 2H), 6.14 (dt, J = 19.8, 9.1 Hz, 1H), 6.05 (s, 1H), 5.86 (br s, 1H), 5.81–5.80 (m, 2H), 5.31 (t, J = 8.6 Hz, 1H), 5.10 (br s, 2H), 4.38 (dd, J = 12.5, 6.0 Hz, 1H), 4.03 (dd, J = 13.0 Hz, 2.5 Hz, 1H), 3.91–3.88 (m, 1H), 2.12 (s, 3H), 2.06



(s, 3H), 2.04 (s, 6H). ^{13}C NMR (125 MHz, CDCl_3) δ 170.6, 169.7, 169.5, 155.7, 151.9, 141.7, 135.9, 133.2, 133.0, 132.7, 129.6, 126.3, 124.7, 123.3, 122.5, 100.5, 83.5, 72.8, 68.7, 68.0, 66.2, 61.5, 45.6, 20.7, 20.7. ^{13}C - ^{19}F couplings in ^{13}C NMR: (125 MHz, CDCl_3) δ 132.9 (q, $J_{\text{C-F}} = 32.76$ Hz, C_2), 126.3 (d, $J_{\text{C-F}} = 3.78$ Hz, C_3), 123.6 (q, $J_{\text{C-F}} = 273.42$ Hz, C_1). HRMS (ESI-TOF), m/z calcd. $\text{C}_{30}\text{H}_{30}\text{F}_3\text{N}_6\text{O}_{10}$ $[\text{M} + \text{H}]^+$ 691.1970; found: 691.2318.

4.2.25 (2R,3R,4S,5S,6S)-2-(Acetoxymethyl)-6-(4-((5-(4-isopropylphenyl)-7-oxopyrazolo[1,5-a]pyrimidin-1(7H)-yl)methyl)-1H-1,2,3-triazol-1-yl)tetrahydro-2H-pyran-3,4,5-triyl triacetate (46). Off-white colored sticky solid; yield: 119.98 mg (94%), $R_f = 0.22$ (ethyl acetate); ^1H NMR (500 MHz, CDCl_3) δ 7.75 (s, 2H), 7.41 (d, $J = 8.4$ Hz, 2H), 7.35 (d, $J = 8.6$ Hz, 2H), 6.10 (s, 1H), 6.03 (s, 1H), 5.89–5.81 (m, 2H), 5.80 (s, 1H), 5.31 (t, $J = 8.7$ Hz, 1H), 5.17 (s, 2H), 4.35 (dd, $J = 12.8$, 5.6 Hz, 1H), 4.01 (dd, $J = 12.0$ Hz, 2.5 Hz, 1H), 3.90–3.86 (m, 1H). 2.97 (hept, $J = 7.1$ Hz, 1H), 2.11 (s, 3H), 2.04 (s, 3H), 2.02 (s, 6H), 1.28 (d, $J = 6.8$ Hz, 6H). ^{13}C NMR (125 MHz, CDCl_3) δ 170.5, 169.6, 169.4, 156.1, 153.7, 151.9, 142.4, 129.8, 128.7, 127.3, 123.2, 100.1, 83.5, 72.6, 68.7, 68.1, 66.2, 61.5, 45.6, 34.1, 23.8, 20.7, 20.6. HRMS (ESI-TOF), m/z calcd. $\text{C}_{32}\text{H}_{37}\text{N}_6\text{O}_{10}$ $[\text{M} + \text{H}]^+$ 665.2566; found: 665.2900.

4.2.26 (2R,3R,4S,5S,6S)-2-(Acetoxymethyl)-6-(4-((5-(naphthalen-2-yl)-7-oxopyrazolo[1,5-a]pyrimidin-1(7H)-yl)methyl)-1H-1,2,3-triazol-1-yl)tetrahydro-2H-pyran-3,4,5-triyl triacetate (47). Off-white colored powder; yield: 123.57 mg (96%), $R_f = 0.23$ (ethyl acetate); ^1H NMR (500 MHz, CDCl_3) δ 8.02 (s, 1H), 7.98 (d, $J = 8.7$ Hz, 1H), 7.92 (d, $J = 7.4$ Hz, 2H), 7.80 (s, 1H), 7.74 (s, 1H), 7.60 (p, $J = 7.4$ Hz, 2H), 7.55 (d, $J = 8.8$ Hz, 1H), 6.16 (s, 1H), 6.02 (d, $J = 2.7$ Hz, 1H), 5.90 (br s, 1H), 5.87 (t, $J = 4.0$ Hz, 1H), 5.82 (dd, $J = 9.0$ Hz, 3.5 Hz, 1H), 5.31 (t, $J = 8.5$ Hz, 1H), 5.19 (br s, 2H), 4.36 (dd, $J = 12.5$, 5.5 Hz, 1H), 4.01 (dd, $J = 12.0$ Hz, 2.0 Hz, 1H), 3.89–3.85 (m, 1H). 2.11 (s, 3H), 2.05 (s, 3H), 2.03 (s, 3H), 2.01 (s, 3H). ^{13}C NMR (125 MHz, CDCl_3) δ 170.5, 169.6, 169.4, 156.0, 153.5, 143.5, 143.2, 142.2, 133.8, 132.8, 129.7, 129.2, 129.0, 128.6, 128.0, 127.6, 125.1, 123.2, 100.5, 90.9, 83.5, 72.6, 68.7, 68.1, 66.2, 61.5, 45.6, 20.7. HRMS (ESI-TOF), m/z calcd. $\text{C}_{33}\text{H}_{33}\text{N}_6\text{O}_{10}$ $[\text{M} + \text{H}]^+$ 673.2253; found: 673.2583.

4.2.27 (2R,3R,4S,5S,6S)-2-(Acetoxymethyl)-6-(4-((5-(benzo[d][1,3]dioxol-5-yl)-7-oxopyrazolo[1,5-a]pyrimidin-1(7H)-yl)methyl)-1H-1,2,3-triazol-1-yl)tetrahydro-2H-pyran-3,4,5-triyl triacetate (48). Off-white colored sticky solid; yield: 121.43 mg (93%), $R_f = 0.22$ (ethyl acetate); ^1H NMR (500 MHz, CDCl_3) δ 7.82 (s, 1H), 7.74 (s, 1H), 6.99–6.94 (m, 2H), 6.91 (d, $J = 8.0$ Hz, 1H), 6.08 (s, 1H), 6.05 (s, 3H), 5.87 (br s, 1H), 5.81 (dd, $J = 9.0$ Hz, 3.5 Hz, 1H), 5.77 (br s, 1H), 5.30 (t, $J = 8.5$ Hz, 1H), 5.18 (br s, 2H), 4.35 (dd, $J = 12.5$, 6.0 Hz, 1H), 4.01 (dd, $J = 12.0$ Hz, 2.5 Hz, 1H), 3.89–3.86 (m, 1H). 2.10 (s, 3H), 2.04 (s, 3H), 2.02 (s, 6H). ^{13}C NMR (125 MHz, CDCl_3) δ 170.5, 169.6, 169.4, 156.0, 153.1, 149.6, 148.3, 143.4, 143.1, 142.3, 125.8, 123.3, 123.1, 109.0, 102.0, 100.2, 90.9, 83.5, 72.6, 68.7, 68.0, 66.2, 61.5, 45.6, 20.7, 20.6. HRMS (ESI-TOF), m/z calcd. $\text{C}_{30}\text{H}_{31}\text{N}_6\text{O}_{12}$ $[\text{M} + \text{H}]^+$ 667.1994; found: 667.2340.

4.3. Cell culture

MDA-MB-231, a human breast cancer cell line, was cultured under standard conditions. Specifically, they were grown in

Dulbecco's Modified Eagle's Medium (DMEM) supplemented with 10% heat-inactivated Fetal Bovine Serum (FBS) and 1% penicillin-streptomycin. The cells were maintained as a monolayer in a 100 mm culture plate and were used for experiments before reaching their 8th passage. Subculturing was performed every third day using trypsin EDTA treatment. All incubation and maintenance procedures were carried out in a humidified CO_2 incubator at 37 °C.

4.4. Cell viability assay

To evaluate cell viability, the MTT assay was conducted following standard procedures. After 72 hours of cell incubation with or without each compound, cell viability was assessed using MTT (3-(4,5-dimethylthiazol-2-yl)-2,5-diphenyltetrazolium bromide), which is a colorimetric method for determining the number of viable cells in various assays including proliferation, cytotoxicity, or chemosensitivity. The MTT reagent was added to the cells after removal of the medium and incubated for 3 hours at 37 °C in the CO_2 incubator. The formazan product, which is soluble in the tissue culture medium, was dissolved in DMSO, and the absorbance of the formazan product was directly measured at 595 nm using a multimode plate reader without additional processing. The absorbance values are directly proportional to the number of viable cells in culture. The percentage of viable cells in each group was determined relative to the untreated control cells.

4.5. Docking analysis

The docking studies were carried out using various derived triazole bridged *N*-glycosides of pyrazolo[1,5-*a*]pyrimidinone with proposed binding pocket of X-ray crystallographic structure (Protein Data Bank ID: 1A52, resolution: 2.6 Å). Docking was performed using Autodock Vina 4.0, and the interaction between the ligands and protein after docking was visualized and analyzed using PyMol software. The Biovia Discovery Studio Visualizer v20.1.0.19295 was used for 2D visualization and detailed ligand interaction visualization. The Schrödinger Maestro tool was utilized for QSAR and SAR studies.

Conflicts of interest

There are no conflicts to declare.

Acknowledgements

The authors are thankful to Banaras Hindu University (BHU) and Jawaharlal Nehru University (JNU) for providing research facilities to carry out this work. GT and AK are thankful to Banaras Hindu University (BHU) for Institute Fellowships. VKM and SS are thankful to UGC New Delhi for JRF/SRF Fellowships.

References

- 1 C. T. Walsh, *Tetrahedron Lett.*, 2015, **56**, 3075–3081.
- 2 A. Arias-Gómez, A. Godoy and J. Portilla, *Molecules*, 2021, **26**, 2708.



- 3 P. K. Sharma, A. Amin and M. Kumar, *Open J. Med. Chem.*, 2020, **14**, 49–64.
- 4 Y. V. Burgart, N. A. Elkina, E. V. Shchegolkov, O. P. Krasnykh, V. V. Maslova, G. A. Triandafilova, S. Y. Solodnikov, G. F. Makhaeva, O. G. Serebryakova, E. V. Rudakova and V. I. Saloutin, *Chem. Heterocycl. Compd.*, 2020, **56**, 199–207.
- 5 J. A. Markwalder, M. R. Arnone, P. A. Benfield, M. Boisclair, C. R. Burton, C.-H. Chang, S. S. Cox, P. M. Czerniak, C. L. Dean, D. Doleniak, R. Grafstrom, B. A. Harrison, R. F. Kaltenbach, D. A. Nugiel, K. A. Rossi, S. R. Sherk, L. M. Sisk, P. Stouten, G. L. Trainor, P. Worland and S. P. Seitz, *J. Med. Chem.*, 2004, **47**, 5894–5911.
- 6 P. Singla, V. Luxami and K. Paul, *RSC Adv.*, 2014, **4**, 12422–12440.
- 7 R. N. Rao and K. Chanda, *Bioorg. Chem.*, 2020, **99**, 103801.
- 8 S. Pinheiro, E. M. C. Pinheiro, E. M. F. Muri, J. C. Pessôa, M. A. Cadorini and S. J. Greco, *Med. Chem. Res.*, 2020, **29**, 1751–1776.
- 9 R. Sagar, M.-J. Kim and S. B. Park, *Tetrahedron Lett.*, 2008, **49**, 5080–5083.
- 10 R. Sagar and S. B. Park, *J. Org. Chem.*, 2008, **73**, 3270–3273.
- 11 C. Narayana, P. Kumari, D. Ide, N. Hoshino, A. Kato and R. Sagar, *Tetrahedron*, 2018, **74**, 1957–1964.
- 12 C. Narayana, P. Kumari and R. Sagar, *Org. Lett.*, 2018, **20**, 4240–4244.
- 13 C. Narayana, A. Khanna, P. Kumari and R. Sagar, *Asian J. Org. Chem.*, 2021, **10**, 392–399.
- 14 P. K. Singh, in *Fused Pyrimidine-Based Drug Discovery*, ed. R. Kumar and R. Vardanyan, Elsevier, 2023, pp. 273–332, DOI: [10.1016/B978-0-443-18616-5.00010-7](https://doi.org/10.1016/B978-0-443-18616-5.00010-7).
- 15 A. Kumar, K. K. Bhagat, A. K. Singh, H. Singh, T. Angre, A. Verma, H. Khalilullah, M. Jaremko, A.-H. Emwas and P. Kumar, *RSC Adv.*, 2023, **13**, 6872–6908.
- 16 J. Castillo and J. Portilla, *Targets Heterocycl. Syst.*, 2018, **22**, 194–223.
- 17 A. Khanna, P. Dubey and R. Sagar, *Curr. Org. Chem.*, 2021, **25**, 2378–2456.
- 18 P. Kumari, S. Dubey, S. Venkatachalapathy, C. Narayana, A. Gupta and R. Sagar, *New J. Chem.*, 2019, **43**, 18590–18600.
- 19 P. Kumari, S. Gupta, C. Narayana, S. Ahmad, N. Vishnoi, S. Singh and R. Sagar, *New J. Chem.*, 2018, **42**, 13985–13997.
- 20 P. Kumari, V. S. Mishra, C. Narayana, A. Khanna, A. Chakrabarty and R. Sagar, *Sci. Rep.*, 2020, **10**, 6660.
- 21 V. K. Mishra, G. Tiwari, A. Khanna, R. Tyagi and R. Sagar, *Synthesis*, 2023, **55**, DOI: [10.1055/a-2157-9100](https://doi.org/10.1055/a-2157-9100).
- 22 A. Khanna, G. Tiwari, V. K. Mishra, K. Singh and R. Sagar, *Synthesis*, 2023, **55**, DOI: [10.1055/a-2181-9709](https://doi.org/10.1055/a-2181-9709).
- 23 R. W. Gantt, P. Peltier-Pain, S. Singh, M. Zhou and J. S. Thorson, *Proc. Natl. Acad. Sci. U. S. A.*, 2013, **110**, 7648–7653.
- 24 Y.-S. Lin, R. Tungpradit, S. Sinchaikul, F.-M. An, D.-Z. Liu, S. Phutrakul and S.-T. Chen, *J. Med. Chem.*, 2008, **51**, 7428–7441.
- 25 D.-Z. Liu, S. Sinchaikul, P. V. G. Reddy, M.-Y. Chang and S.-T. Chen, *Bioorg. Med. Chem. Lett.*, 2007, **17**, 617–620.
- 26 K. R. Hande, *Eur. J. Cancer*, 1998, **34**, 1514–1521.
- 27 H. Stähelin and A. Von Wartburg, *Prog. Drug Res.*, 1989, 169–266.
- 28 M. Gui, D.-K. Shi, M. Huang, Y. Zhao, Q.-M. Sun, J. Zhang, Q. Chen, J.-M. Feng, C.-H. Liu, M. Li, Y.-X. Li, M. Geng and J. Ding, *Invest. New Drugs*, 2011, **29**, 800–810.
- 29 J. Kluza, R. Mazinghien, H. Irwin, J. A. Hartley and C. Bailly, *Anti-Cancer Drugs*, 2006, **17**, 155–164.
- 30 E. C. Calvaresi and P. J. Hergenrother, *Chem. Sci.*, 2013, **4**, 2319–2333.
- 31 A. Shivappagowdar, S. Pati, C. Narayana, R. Ayana, H. Kaushik, R. Sah, S. Garg, A. Khanna, J. Kumari, L. Garg, R. Sagar and S. Singh, *Dis. Models Mech.*, 2019, **12**, dmm040410.
- 32 S. Gupta, J. Khan, P. Kumari, C. Narayana, R. Ayana, M. Chakrabarti, R. Sagar and S. Singh, *Malar. J.*, 2019, **18**, 346.
- 33 K. Singh, R. Tyagi, V. K. Mishra, G. Tiwari and R. Sagar, *SynOpen*, 2023, **07**, 322–352.
- 34 A. K. Agrahari, P. Bose, M. K. Jaiswal, S. Rajkhowa, A. S. Singh, S. Hotha, N. Mishra and V. K. Tiwari, *Chem. Rev.*, 2021, **121**, 7638–7956.
- 35 K. Cheng, Q.-X. Bai, S.-J. Hu, X.-Q. Guo, L.-P. Zhou, T.-Z. Xie and Q.-F. Sun, *Dalton Trans.*, 2021, **50**, 5759–5764.
- 36 J. Huo, H. Hu, M. Zhang, X. Hu, M. Chen, D. Chen, J. Liu, G. Xiao, Y. Wang and Z. Wen, *RSC Adv.*, 2017, **7**, 2281–2287.
- 37 C. Narayana, P. Kumari, G. Tiwari and R. Sagar, *Langmuir*, 2019, **35**, 16803–16812.
- 38 S. Shah, A. G. Dalecki, A. P. Malalasekera, C. L. Crawford, S. M. Michalek, O. Kutsch, J. Sun, S. H. Bossmann and F. Wolschendorf, *Antimicrob. Agents Chemother.*, 2016, **60**, 5765–5776.
- 39 D. A. Iovan, S. Jia and C. J. Chang, *Inorg. Chem.*, 2019, **58**, 13546–13560.
- 40 R. Sagar, J. Park, M. Koh and S. B. Park, *J. Org. Chem.*, 2009, **74**, 2171–2174.
- 41 J. Ren, S. Ding, X. Li, R. Bi and Q. Zhao, *J. Org. Chem.*, 2021, **86**, 12762–12771.
- 42 C. Almansa, A. F. de Arriba, F. L. Cavalcanti, L. A. Gómez, A. Miralles, M. Merlos, J. Garcia-Rafanell and J. Forn, *J. Med. Chem.*, 2001, **44**, 350–361.
- 43 J.-C. Castillo, D. Estupiñan, M. Nogueras, J. Cobo and J. Portilla, *J. Org. Chem.*, 2016, **81**, 12364–12373.
- 44 G. Tiwari, A. Khanna, R. Tyagi, V. K. Mishra, C. Narayana and R. Sagar, *Sci. Rep.*, 2023, 50202.

